Any correspondence concerning this service should be sent to the repository administrator: tech-oatao@listes-diff.inp-toulouse.fr

Hydrodynamic Study of a Circulating Fluidized Bed at High Temperatures: Application to Biomass Gasification [†]

Sébastien Pecate[1*], Mathieu Morin[1], Sid Ahmed Kessas[1], Mehrdji Hemati[1], Yilmaz Kara[2] and Sylvie Valin[3]

[1] Laboratoire de Génie Chimique, Université de Toulouse, France
[2] ENGIE Lab - Centre de Recherche et d'Innovation Gaz et Energies Nouvelles (CRIGEN), France
[3] CEA (LITEN), France

Abstract

Experimental data on the hydrodynamic behavior of dense and circulating fluidized beds at high temperatures are scarce in the literature. This work deals with the hydrodynamic study of a Fast Internally Circulating Fluidized Bed (FICFB) used for biomass gasification. The first part of this study investigates the influence of the bed temperature (between 20 and 950 °C) and the nature of fluidizing gas (air or steam) on the hydrodynamic parameters of a dense fluidized bed of olivine particles (i.e. minimum fluidization velocity and voidage as well as average voidage). Three olivine batches are used with a mean Sauter diameter of 282, 464 and 689 µm, respectively. Experimental results are compared with different empirical correlations from the literature to evaluate their validity under elevated temperature conditions. Besides, two dimensionless correlations calculating the minimum fluidization velocity and average bed voidage are proposed. The second part of this study focuses on the hydrodynamic behavior of an FICFB operating between 20 and 850 °C. The effect of different process parameters (i.e. bed material nature, air velocity, solids inventory, bed temperature) on the solids circulation flow rate is investigated. It was found that the transport velocity U_{tr} is not affected by the bed temperature and the bed material inventory. It mainly depends on the terminal settling velocity U_t of bed material particles. Besides, key parameters controlling solids flow rate are the combustor gas velocity and the solids inventory. An increase in these parameters leads to a higher circulation flow rate.

Keywords: circulating fluidized bed, transport velocity, hydrodynamic, olivine, biomass gasification

1. Introduction

High-temperature biomass gasification is a promising alternative to fossil fuel for power generation and the production of fuel via methanation or the Fisher-Tropsch process. The reactive system of biomass conversion is an endothermic process. To maintain a fixed temperature in the reactor, a contribution of energy is required. Two types of technology exist for biomass gasification depending on the method of heat transmission (Gómez-Barea and Leckner, 2010; Ruiz et al., 2013). On the one hand, the heat can be provided by "in-situ" combustion. This process includes the fixed bed gasifiers (up-draft and down-

draft) and the "bubbling fluidized bed" gasifiers. In these types of reactors, the biomass undergoes drying, pyrolysis, partial combustion of volatile matters and char and finally gasification of char. On the other hand, the heat can be supplied by the "ex-situ" combustion of char. One of the most promising technologies using "ex-situ" combustion is the Fast Internally Circulating Fluidized Bed (FICFB) (Hofbauer et al., 2002). The facility used in this study is of FICFB type. Its principle relies on the circulation of a medium (sand, olivine or catalyst particles) acting as a heat carrier between an endothermic reactor and an exothermic reactor. In the first one (called gasifier), which operates at around 750 °C–850 °C, biomass is continuously fed into a dense fluidized bed containing the heat transfer medium (olivine particles) fluidized by superheated steam. The biomass thermochemical conversion leads to the production of synthesis gas and a solid carbonaceous residue called char. Bed material (olivine and unconverted char) is continuously discharged through a dump to a transported fluidized bed reactor called "Combustor" that is fed by preheated combustion air. In this reactor, which operates at around 850 °C–950 °C,

combustion of part of the char coming from the gasifier induces olivine particle heating. At the outlet of the combustor, olivine particles are separated from flue gas by a cyclone and are returned to the gasifier through a standpipe. Thus, the heat needed for endothermic steam-gasification is provided by the ex-situ combustion of residual char. The FICFB biomass gasification efficiency is strongly dependent on a thermal equilibrium between gasification zone and combustion zone. This equilibrium is controlled by the temperature difference and circulating solids flow rate between the two reaction zones. However, this last parameter also depends on the process operating conditions (i.e. bed inventory, gas velocity, bed temperature), and cannot be imposed. Thus, it appears essential to identify the process key parameters which enable control of the circulating medium flow rate.

Besides, it is well known that the hydrodynamic behavior of an FICFB affects heat and mass transfer and therefore the overall reaction rate. In the literature, current knowledge on the hydrodynamic behavior of dense and circulating fluidized beds was essentially acquired at ambient operating conditions and a lack of information is noticed on the effect of temperature.

1.1 Brief review on bubbling fluidized bed hydrodynamic study

Shabanian and Chaouki (2017) recently reviewed the effects of temperature, pressure and interparticle forces on the fluidization characteristics of gas-solid dense fluidized beds for a wide spectrum of particles belonging to group A, B and D of the Geldart classification (Geldart, 1973).

For Geldart class-B particles with no interparticle forces and at atmospheric pressure, the minimum fluidization velocity decreases as the temperature increases (Mii et al., 1973; Pattipati and Wen, 1981; Botterill et al., 1982a; Botterill et al., 1982b; Svoboda et al., 1983; Hartman and Svoboda, 1986; Grace and Sun, 1991; Llop et al., 1995; Formisani et al., 1998). The authors explain this trend by the fact that the increasing viscosity, with a rise in bed temperature, is the controlling factor for class-B particles. Some authors also investigated the effect of mean particle diameter on minimum fluidization velocity (Geldart, 1972; Stubington et al., 1984; Fatah, 1991; Tannous, 1993; Gauthier et al., 1999). The authors agreed to say that minimum fluidization velocity increases with mean particle size. Besides, many authors proposed correlations to estimate the minimum fluidization velocity (Wen and Yu, 1966; Bourgeois and Grenier, 1968; Richardson, 1971; Saxena and Vogel, 1977; Babu et al., 1978; McKay and McLain, 1980; Svoboda et al., 1983; Chitester et al., 1984; Thonglimp et al., 1984; Nakamura et al., 1985; Lucas et al., 1986; Chyang and Huang, 1988; Murachman, 1990;

Fatah, 1991 and Tannous et al., 1994). They are listed in **Table 1**. The correlations proposed were often derived from the Ergun equation (Ergun, 1952) for pressure drop through a packed bed calculation (Equation 1):

$$\frac{\Delta P}{L} = \frac{150 \cdot (1-\varepsilon)^2}{\varepsilon^3} \frac{\mu_f U}{(\varphi d_p)^2} + \frac{1.75 \cdot (1-\varepsilon)}{\varepsilon^3} \frac{\rho_f U^2}{\varphi d_p} \quad (1)$$

where ΔP is the pressure drop (Pa), U is the fluid superficial velocity (m·s^{-1}), ε is the bed average voidage (–), L is the bed height (m), μ_f is the fluid viscosity (Pa·s), φ is the shape factor (–), d_p is the mean particle diameter (m) and ρ_f is the fluid density (kg·m^{-3}).

Considering minimum fluidization as the transitional state between fixed bed and fluidized bed, the pressure drop through the fixed bed, defined in Equation 1, is equal to the bed weight per unit area. By using dimensionless Reynolds and Archimedes numbers, the Ergun equation at minimum fluidization leads to Equation 2:

$$Ar = \frac{150 \cdot (1-\varepsilon_{mf})}{\varphi^2 \cdot \varepsilon_{mf}^3} \cdot Re_{mf} + \frac{1.75}{\varphi \cdot \varepsilon_{mf}^3} \cdot Re_{mf}^2 \quad (2)$$

with:

$$Re_{mf} = \frac{\rho_f \cdot U_{mf} \cdot d_p}{\mu_f} \text{ and } Ar = \frac{g \cdot d_p^3 \cdot \rho_f \cdot (\rho_p - \rho_f)}{\mu_f^2} \quad (3)$$

where Ar is the Archimedes number (–), Re_{mf} is the Reynolds number at minimum fluidization (–), ε_{mf} is the minimum fluidization voidage (–), U_{mf} is the minimum fluidization velocity (m·s^{-1}), g is the acceleration due to gravity (m·s^{-2}) and ρ_p is the particle apparent density (kg·m^{-3}). Equation 2 may be rearranged to Equation 4, where K_1 and K_2 are constant numbers depending on the minimum fluidization voidage and shape factor.

$$Ar = K_1 \cdot Re_{mf} + K_2 \cdot Re_{mf}^2 \quad (4)$$

By solving Equation 4, Re_{mf} can be expressed as a function of Ar (Equation 5).

$$Re_{mf} = (C_1^2 + C_2 \cdot Ar)^{0.5} - C_1 \quad (5)$$

where:

$$C_1 = \frac{K_1}{2 \cdot K_2} \quad \text{and} \quad C_2 = \frac{1}{K_2} \quad (6)$$

Several authors attempted to estimate C_1 and C_2 through experimental data at various operating conditions (**Table 1**). However, studies performed at high temperatures are scarce in the literature. Most of the correlations were established at ambient temperature, as reported in **Table 1**. However, it is known that the bed temperature greatly influences viscosity and density of gas, thus making the use of these correlations a source of errors.

Regarding minimum fluidization voidage, it was found to slightly increase with bed temperature (Botterill et al., 1982a; Botterill et al., 1982c; Llop et al., 1995; Formisani

Table 1 Correlations in the literature for the prediction of minimum fluidization velocity.

Authors	Particle mean diameter (μm)	Particle apparent density (kg·m⁻³)	Shape factor φ (–)	Fluidizing agent	Bed temperature (°C)	Reactor pressure (bar)	Correlations
Tannous et al. (1994)	725–3900	1016–3950	0.62–1	Air	Ambient	1.013	$Re_{mf} = (25.83^2 + 0.043 \cdot Ar)^{0.5} - 25.83$
Wen and Yu (1966)	2050–6350	2360–7840	1	H_2O	Ambient	1.013	$Re_{mf} = (33.7^2 + 0.0408 \cdot Ar)^{0.5} - 33.7$
Bourgeois and Grenier (1968)	86–2510	1200–19300	1	Air and H_2O	Ambient	1.013	$Re_{mf} = (25.46^2 + 0.03824 \cdot Ar)^{0.5} - 25.46$
Richardson (1971)	Spherical and non-spherical particles						$Re_{mf} = (25.7^2 + 0.0365 \cdot Ar)^{0.5} - 25.7$
Saxena and Vogel (1977)	650–704	1900–2460	0.73–0.98	Air	18–427	1.79–8.34	$Re_{mf} = (25.28^2 + 0.0571 \cdot Ar)^{0.5} - 25.28$
Babu et al. (1978)	50–2870	2560–3924	0.63–0.74	Air–CO_2–N_2–H_2O–Chlorofluorocarbon	Ambient	1.013–69.914	$Re_{mf} = (25.25^2 + 0.0651 \cdot Ar)^{0.5} - 25.25$
McKay and McLain (1980)	9486–28690	1140–1490	0.387–0.417	H_2O	Ambient	1.013	$Re_{mf} = \left[(83.33 \cdot (1-\varepsilon_{mf}))^2 + \dfrac{\varepsilon_{mf}^3 \cdot \varphi \cdot Ar}{2.4} \right]^{0.5} - 83.33 \cdot (1-\varepsilon_{mf})$
Svoboda et al. (1983)	565–1125	1680–3330	0.524–0.819	Air	20–890	1.013	$Re_{mf} = \left[\left(\dfrac{28.407 \cdot (1-\varepsilon_{mf})}{\varphi} \right)^2 + \dfrac{\varepsilon_{mf}^3 \cdot \varphi \cdot Ar}{3.392} \right]^{0.5} - \dfrac{28.407 \cdot (1-\varepsilon_{mf})}{\varphi}$
Chitester et al. (1984)	88–374	1116–2472	n.r.	N_2	Ambient	1.013–6.306	$Re_{mf} = (28.7^2 + 0.0494 \cdot Ar)^{0.5} - 28.7$
Thonglimp et al. (1984)	180–2125	1607–7425	1	Air	Ambient	1.013	$Re_{mf} = (31.6^2 + 0.0425 \cdot Ar)^{0.5} - 31.6$
Nakamura et al. (1985)	200–4000	2500	1	N_2	7–527	1–50	$Re_{mf} = (33.95^2 + 0.0465 \cdot Ar)^{0.5} - 33.95$
Lucas et al. (1986)	Correlation from data in literature						$Re_{mf} = (29.5^2 + 0.0357 \cdot Ar)^{0.5} - 29.5$
Chyang and Huang (1988)	699–6062	910–6860		Air–Argon	15–830	1.013	$Re_{mf} = (33.3^2 + 0.0333 \cdot Ar)^{0.5} - 33.3$
Murachman (1990)	109–917	1480–3910	0.77–0.92	Air	20–900	1.013	$Re_{mf} = 0.0016 \cdot Ar^{0.9}$
Fatah (1991)	1000–3570	3950	0.48–0.89	Air	15–725	1.013	$Re_{mf} = \left(-7.987 \times 10^{-3} + \dfrac{16.058}{T} \right) \cdot Ar^{\left(0.5547 + \frac{2.084 \times 10^{-4}}{T} \right)}$

n.r.: non-reported

et al., 1998). Besides, the effect of mean particle size on this parameter is a source of controversy. Through experiments carried out with various bed materials belonging to group A and B of the Geldart classification (coal, sand, glass, coke, ceramic, carborundum, anthracite, cracking catalyst...), different trends were observed (Lewis et al., 1949; Matheson et al., 1949; Agarwal and Storrow, 1951; Van Heerden et al., 1951; Rowe, 1965; Geldart, 1972). When mean particle size increases, minimum fluidization voidage is found: to decrease according to Matheson et al. (1949), Agarwal and Storrow (1951), Rowe (1965), and Geldart (1972), to increase in the work of Van Heerden et al. (1951), and to remain unchanged for Lewis et al. (1949).

Finally, studies about average bed voidage showed that there is no influence of bed temperature for Geldart class-B particles (Botterill et al., 1982a; Botterill et al., 1982c). According to the authors, this parameter only depends on excess gas velocity (U-U_{mf}). The effect of mean particle size on average bed voidage was also investigated with various bed materials (ballotini crystal, cracking catalyst and sand particles) (Lewis et al., 1949; Rowe, 1965; Geldart, 1972). The authors found that the average bed voidage decreases as the mean particle size increases. Besides, several correlations were proposed in order to estimate the average bed voidage (Lewis et al., 1949; Matsen et al., 1969; Thonglimp et al., 1984; Chyang and Huang, 1988; Hilal and Gunn, 2002). These correlations are given in **Table 2**, and were established from experimental data obtained in gas-solid and liquid-solid reactors, or from the two-phase theory assuming that excess gas regarding minimum fluidization crosses the bed as bubbles.

1.2 Brief review on circulating fluidized bed hydrodynamic study

Circulating fluidized bed technologies have been used since 1940 for the Fuel Catalytic Cracking process (FCC) (Lim et al., 1995; Grace et al., 1997). In spite of this, the phenomena involved were not investigated until the 1970s (Yerushalmi et al., 1976). Lim et al. (1995) and Berruti et al. (1995) reported that circulating fluidized bed reactors offer several common advantages compared to conventional low-velocity bubbling and turbulent fluidized bed reactors. These advantages are: favorable gas-solids contact efficiency due to high slip between gas and solids, a more uniform distribution of solids due to reduced gas bypassing, reduced axial gas and solids back-mixing, higher gas throughput, independent gas and solids retention time control, improved turndown and possible separate gaseous reactant zones.

A large number of works in the literature are devoted to the identification of the fluidization regimes in risers. Yerushalmi et al. (1976) focused on the identification of transition velocities between bubbling, plugging and tur-

bulent regimes at ambient temperature for class-A particles of the Geldart classification. The authors highlighted two characteristic velocities, U_c and U_k, which correspond to transition and complete turbulent fluidization velocities, respectively. For a gas velocity lower than U_c, bed pressure drop standard deviation increases to a peak as a result of a bubble coalescence phenomenon. Between U_c and U_k, internal solids circulation yields to bubbles breakup and decreases pressure drop standard deviation. Beyond U_k, the pressure drop standard deviation stabilizes and solid particles begin to be carried in the gaseous flow. These two velocities (i.e. U_c and U_k) are easily measurable for class-A particles but are not well-defined for other class particles. Chehbouni et al. (1994) denied the existence of turbulent velocity U_k for Geldart class-B particles. They concluded that the onset of turbulent fluidization is at U_c, and velocity U_k is an artefact due to the use of differential pressure transducers.

There is more than one technique for measuring the transport velocities of particles. Those recorded in the literature include determination of the flooding point (Yerushalmi and Cankurt, 1979), determination of the pressure drop at the bottom of the column as a function of the solids circulation flux at different gas velocities (Yerushalmi and Cankurt, 1979), determination of the maximum solids circulation flux at different gas velocities (Schnitzlein and Weinstein, 1988), and determination of the emptying times of a fast fluidization column (Han et al., 1985). According to Adanez et al. (1993), the last technique is the most attractive because the measurement is simple and quick to conduct.

By measuring the solids flow rate versus the gas velocity, Yerushalmi and Cankurt (1979) also reported the existence of a characteristic particle transport velocity U_{tr}, which corresponds to the onset of a fully transported bed flow.

Several authors attempted to estimate the influence of column diameter as well as solids properties and hold-up on the transition velocities U_c, U_k and U_{tr} at ambient temperature (Fan et al., 1983; Han et al., 1985; Mori et al., 1986; Lee and Kim, 1990; Perales et al., 1991b; Bi and Fan, 1992; Adanez et al., 1993; Tannous, 1993; Chehbouni et al., 1995). Most authors concluded that turbulent transition velocities increase with column diameter, for the same solids static height (Rhodes and Geldart, 1986; Grace and Sun, 1991; Chehbouni et al., 1995). This phenomenon is attributed to the effect of column diameter on bubble size. For a given gas velocity, an increase in column diameter leads to the formation of smaller bubbles which reduces internal solids circulation in the bed and delays the onset of the turbulent regime. Transport velocity U_{tr} also increases with column diameter. The solids static height was found to have a very low influence on turbulent transition and transport velocities (Werther,

Table 2 Correlations in the literature for the prediction of average bed voidage.

Authors	Particle mean diameter (μm)	Particle apparent density (kg·m⁻³)	Shape factor φ (−)	Fluidizing agent	Bed temperature (°C)	Reactor pressure (bar)	Correlations
Thonglimp et al. (1984)	180–2125	1600–7425	1	Air	Ambient	1.013	$\varepsilon = 1.57 \cdot Re^{0.29} \cdot Ar^{-0.19}$
Chyang and Huang (1988)	699–6062	910–6860	n.r.	Air–Argon	Ambient	1.013	$\varepsilon = 1.05 \cdot Re^{0.30} \cdot Ar^{-0.17}$
Lewis et al. (1949)	100–570	n.r.	n.r.	H_2O	Ambient	1.013	$\dfrac{H}{H_{mf}} = 1 + \dfrac{0.0034 \cdot (U - U_{mf})}{d_p^{0.5}}$
Matsen et al. (1969)	Two-phase theory						$\dfrac{H}{H_{mf}} = 1 + \dfrac{U - U_{mf}}{0.35 \cdot (g \cdot Dc)^{0.5}}$
Hilal and Gunn (2002)	50–1000	1228–11400	n.r.	Air	Ambient	1.013	$\dfrac{\rho_b}{\rho_{mf}} = \exp\left(-0.0052 \cdot U_t \cdot \left(\dfrac{\rho_f}{\mu_f \cdot g}\right)^{1/3} \cdot \left(\dfrac{U}{U_{mf}} - 1\right)\right)$

n.r.: non-reported

Table 3 Correlations in the literature for the prediction of characteristic U_{tr} velocity.

Authors	Operating conditions at which the correlations were established				Correlations
	Particle mean diameter (μm)	Particle apparent density (kg·m⁻³)	Fluidizing agent	Bed temperature	Class of particles	

Authors	Particle mean diameter (μm)	Particle apparent density (kg·m⁻³)	Fluidizing agent	Bed temperature	Class of particles	Correlations
Mori et al. (1986)	56–134	729–2400	—	—	B	$Re_{tr} = 1.41 \cdot Ar^{0.56}$
Lee and Kim (1990)	24–205	1250–2500	Air	Ambient	B	$Re_{tr} = 2.916 \cdot Ar^{0.354}$
Perales et al. (1991b)	325–975	2650	Air	Ambient	B	$Re_{tr} = 1.41 \cdot Ar^{0.483}$
Perales et al. (1991a)	n.r.	n.r.	Ambient	Ambient	B	$U_{tr} = 1.7 \cdot U_t$
Bi and Fan (1992)	325	660	Air	Ambient	B	$Re_{tr} = 2.28 \cdot Ar^{0.419}$
Adanez et al. (1993)	80–900	1400–2600	Air	Ambient	B	$Re_{tr} = 2.078 \cdot Ar^{0.463}$
Tannous (1993)	715–2800	1016–2650	Air	Ambient	B	$Re_{tr} = 1.834 \cdot Ar^{0.448}$
Ryu et al. (2003)	181	4080	Air	25–600	B	$Re_{tr} = 0.0428 \cdot Ar^{0.5866} \cdot \left(\dfrac{Dc}{d_p}\right)^{0.5208}$
Chehbouni et al. (1995)	23.6–5000	660–4510	Air	Ambient	A, B, C and D	$Re_{tr} = 0.169 \cdot Ar^{0.545} \cdot \left(\dfrac{Dc}{d_p}\right)^{0.3}$
Goo et al. (2010)	210–380	2500	Air	20–600	B	$Re_{tr} = 2.001 \cdot Ar^{0.405}$

1974; Satija and Fan, 1985; Chehbouni et al., 1995). Moreover, an increase in particle size and density leads to higher transition characteristic velocities U_c and U_k and transport velocity U_{tr} (Cai et al., 1990; Chehbouni et al., 1995). Lee and Kim (1990) showed that the transition turbulent fluidization velocity U_c is almost equal to the terminal settling velocity of single particles U_t for class-B particles. Furthermore, very recent studies have proved that the particle size distribution (PSD) has an influence on the transition velocity U_c, which was found to be higher for materials with a wider PSD (Chehbouni et al., 1995; Rim and Lee, 2016). Experimental data showing the influence of bed temperature on transition velocities are scarce in the literature. According to Bi and Grace (1996), a rise in temperature might cause a shift towards lower transition velocities. Besides, some correlations were proposed in the literature in order to estimate the transport velocity U_{tr} (Mori et al., 1986; Lee and Kim, 1990; Perales et al., 1991a; Perales et al., 1991b; Bi and Fan, 1992; Adanez et al., 1993; Tannous, 1993; Chehbouni et al., 1995; Ryu et al., 2003; Goo et al., 2010). These correlations are reported in **Table 3**, and were established at ambient temperature, for air as the fluidizing agent and for class-B particles.

By varying the gas velocity for a fixed circulating solids flow rate, Yates (1996) and Shamlou (2013) defined a characteristic velocity called choking velocity U_{ch}. It corresponds to the transition between dense phase flow and dilute phase flow. These authors showed that U_{ch} increases with particle size and circulating solids flow rate.

Basu and Cheng (2000) investigated the influence of operating parameters on the performance of a CFB equipped with a loop seal. This work was performed at ambient temperature with sand particles ($dp = 250\ \mu m$). The authors showed that a rise in both the total weight of solid particles in the process (inventory) and the loop seal air velocity leads to an increase in the circulating solids flow rate. Besides, studies carried out by Bull (2008) and Detournay (2011) focused on the hydrodynamic of a circulating fluidized bed biomass gasifier at ambient temperature using olivine ($dp = 250\ \mu m$) and sand particles ($dp = 316\ \mu m$) as media. Results showed that gas velocity in the riser (combustor) and total inventory are the main parameters which influence the circulating solids flow rate.

The present work is divided into two parts. The first part aims to determine the influence of operating conditions such as bed temperature (ranging from 20 to 950 °C), mean particle size (between 282 and 689 μm) and fluidizing gas nature (air or steam) on the hydrodynamic parameters of a dense fluidized bed of olivine particles (i.e. minimum fluidization velocity and voidage as well as average voidage). The purpose of the second part is to identify the key parameters controlling the circulating solids flow rate, as well as their effect on solids circulation.

2. Materials

2.1 Description of the experimental rig

All the experiments were conducted in the FICFB presented below (**Fig. 1**). The process contains two reactors
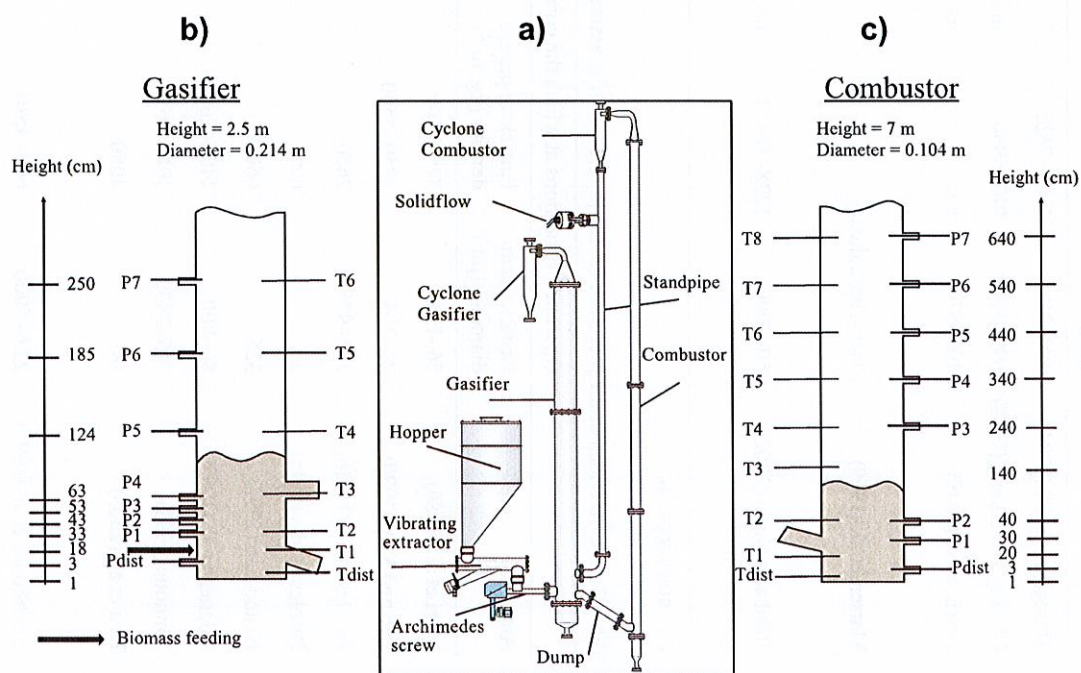

Fig. 1 Circulating fluidized bed biomass gasifier (**a**: pilot plant; **b** and **c**: pressure and temperature tap positions in the gasification section and in the combustion section, respectively).
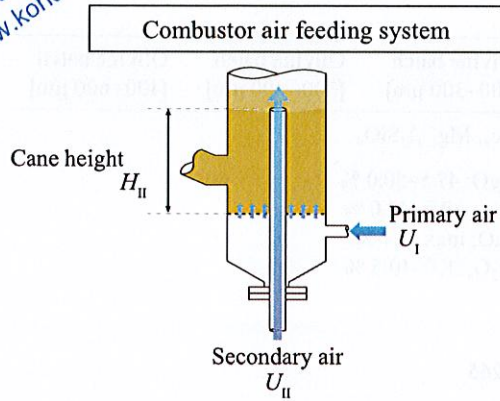
Fig. 2 Distribution of combustion air in the combustor.

whose connections enable an interchange of solids. The gasifier (internal diameter = 214 mm) is a dense fluidized bed of bed material particles. For this hydrodynamic study, it is fluidized either by super-heated steam or by air. The bed material is continuously discharged from the gasifier to the combustor through a dump. The combustor (internal diameter = 104 mm) is a transported fluidized bed, fed by preheated air separated into two streams (**Fig. 2**). The first one, named "primary air", ensures a dense fluidized bed at the bottom of the combustor. The second stream, called "secondary air", is used for particle transport. It is fed by an injection cane at an adjustable height. At the top of the combustor, a cyclone is used to separate transported particles from air. Then, solids are recycled back to the gasifier through the standpipe, equipped with an L-valve placed on the base and fluidized by steam or air.

Gasifier and combustor are surrounded by electric furnaces with 15 and 5.7 kW electric output, respectively. Gasifier and combustor temperatures can be controlled independently by two PID controllers. Nevertheless, carrying out tests at temperatures higher than 500 °C also requires the use of natural gas feeding in the combustor, precisely at 40 cm above the distributor.

The pilot plant is equipped with 23 pressure sensors and 20 temperature sensors (**Fig. 1**). The circulating solids mass flow rate is measured with a microwave probe (supplier: SWR Engineering, model: SolidFlow 2.0), previously calibrated, located in the standpipe, 50 cm below the base of the combustor cyclone (**Fig. 1**).

At the outlet of each reactor, a burner associated with a post-combustion chamber heated to 850 °C allows the burning of all combustible gas. Then, gas streams are mixed together in a cylindrical chamber and cooled down in a 5-m multitubular exchanger. A cyclone and a bag filter ensure the filtration of fine particles before rejecting gas into the atmosphere.

2.2 Bed material pretreatment and characterization

Most of the experiments presented in this study were carried out with olivine particles provided by the Austrian manufacturer Magnolithe GmbH as bed material. Nevertheless, some tests were also performed with sand particles. As shown in **Table 4**, olivine particles are essentially made of magnesium oxide, silicon oxide and iron oxide. The latter reaches 10.5 wt% in our case. Regarding sand particles, they are mainly made of silicon oxide. Before their use as bed material in the gasifier, the particles previously underwent:

- A fine elutriation step. In this step, the undesired fine particles are removed by elutriation, at ambient temperature during 20 hours;
- a calcination step, at 850 °C during 4 hours.

During these stages, carried out in the gasifier, the gas velocity was maintained at 8 times the minimum fluidization velocity ($U = 8 \cdot U_{mf}$) at the considered temperature. After this treatment, the particle size distribution, particle density, skeletal density, aerated bulk density, packed bulk density, angle of repose, internal voidage, specific surface area and shape factor were measured using Laser Diffraction Particle Sizing MS2000, Mercury Porosimetry, Hosokawa analyzer, Helium Pycnometry, BET analyzer and G3 Morphology, respectively. Based on the values of the mean Sauter diameter and particle density reported in **Table 4** for both sand and olivine, it can be concluded that the particles used in this work belong to the Geldart class B. Besides, the particles have a low compressibility factor γ (lower than 15 %), meaning that they have an excellent flow. Otherwise, the particles employed are minimally porous, with internal voidage of 9 % and 7 % for sand and olivine particles, respectively.

In this work, Sauter diameter ($d_{3/2}$) is considered as the mean particle size.

3. Bubbling fluidized bed hydrodynamic study

This part of the study focusses on the effect of bed temperature, particle size distribution and fluidization gas nature (air or steam) on minimum fluidization velocity (U_{mf}) and bed voidage (ε_{mf}), as well as on average voidage (ε) of the olivine particle dense fluidized bed. Experiments are performed in the gasifier, isolated from the combustor and the circulation loop. For each test, the total olivine particle inventory in the gasifier is 40 kg. In addition, some tests are carried out in the combustor, isolated from the gasifier and the circulation loop, in order to confirm the conclusions drawn in the gasifier for a reactor with a different diameter. For each test performed in the combustor, the total olivine inventory is 7 kg.

Table 4 Physical properties of olivine and sand particles.

Type of particle	Sand	Olivine batch [200–300 μm]	Olivine batch [300–400 μm]	Olivine batch [400–600 μm]
Chemical formula	SiO_2	$(Fe_x, Mg_{1-x})_2SiO_4$		
Composition	SiO_2: 98.34 %	MgO: 47.5–50.0 %		
	Fe_2O_3: 0.022 %	SiO_2: 39.0–42.0 %		
	Al_2O_3: 1.206 %	CaO: max. 0.4 %		
	TiO_2: 0.03 %	Fe_2O_3: 8.0–10.5 %		
	CaO: 0.014 %			
	K_2O: 0.745 %			
Skeletal density ρ_s (kg·m^{-3})	2,650	3,265		
Internal voidage χ (%)	9	7		
Particle density ρ_P (kg·m^{-3})	2,400	2,965		
Aerated bulk density ρ_{BA} (kg·m^{-3})	1,519	1,344	1,368	1,445
Packed bulk density ρ_{BP} (kg·m^{-3})	1,643	1,500	1,513	1,643
Mean aerated bulk bed voidage ε_{BA} (–)	0.49	0.53		
Mean packed bulk bed voidage ε_{BP} (–)	0.45	0.48		
Angle of repose (°)	33.2	29.6	—	—
Compressibility factor: $\gamma = 100 \cdot (\rho_{BP}-\rho_{BA})/\rho_{BP}$ (%)	8	10	10	12
Shape factor (–)	0.85	0.85	—	—
d_{10} (μm)	190	188	337	508
d_{50} (μm)	305	300	483	709
d_{90} (μm)	488	475	689	1,015
$d_{3/2}$ (μm)	285	282	464	689
$d_{4/3}$ (μm)	324	318	501	741
$C_v = (d_{90}-d_{10})/d_{50}$ (–)	0.98	0.96	0.73	0.72
Specific surface area (m^2·g^{-1})	—	0.73	—	—

3.1 Determination methods

For each experiment, the bed was first vigorously fluidized and the pressures along the reactor were measured. Then, the gas velocity was decreased and the pressures were measured again. From the experimental results, the minimum fluidization velocity was estimated through (Botterill et al., 1982a; Murachman, 1990; Fatah, 1991; Tannous, 1993):

- the plot of the average total bed pressure against the superficial gas velocity (**Fig. 3a**). As long as the bed is in a fixed state, the total pressure increases with the gas velocity. When the minimum fluidization point is exceeded, the total pressure remains constant as the gas velocity increases. Thus, the intersection of the sloping fixed bed and horizontal fluidized bed pressure lines on the pressure drop versus gas velocity plot was considered as the minimum fluidization velocity;
- the plot of the partial pressure drop, measured be-

tween two pressure sensors, against the superficial gas velocity (**Fig. 3b**). For an increase in the gas velocity, the partial pressure drop first increases as long as the bed is fixed. Then, it slightly decreases as soon as the bed is fluidized. This decrease is related to the rise in the bubble volume fraction in the area considered. Thus, the minimum fluidization velocity can be defined as the peak on the partial pressure drop versus gas velocity plot;
- the plot of the total pressure standard deviation against the superficial gas velocity (**Fig. 3c**). In this study, the standard deviation of a given parameter is defined as below:

$$\sigma_Z = \frac{\left[\frac{1}{N_e - 1} \cdot \sum_{i=1}^{N_e} (Z_i - \overline{Z})^2 \right]^{0.5}}{\overline{Z}} \quad (7)$$

where σ_Z is the standard deviation of the parameter Z, N_e is the number of data, Z_i is the value of Z at a given time, and $\overline{Z}$ is the mean value of Z. For fixed
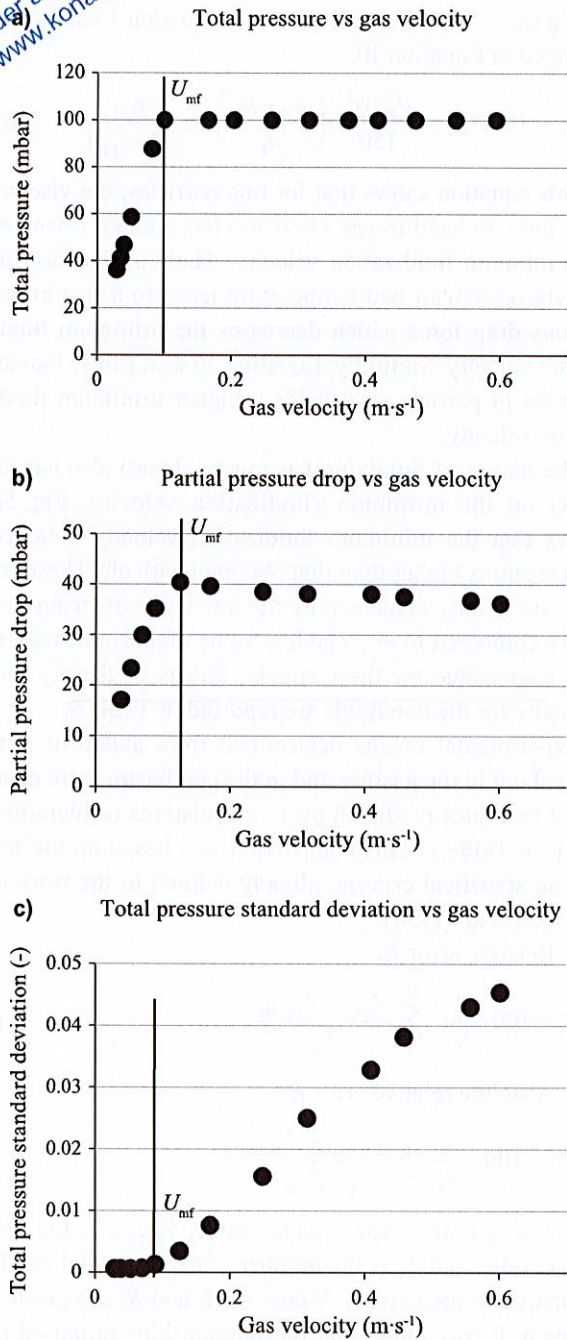
a)

Total pressure vs gas velocity

b)

Partial pressure drop vs gas velocity

c)

Total pressure standard deviation vs gas velocity

Fig. 3 Methods used for the determination of U_{mf}.

a)

Axial pressure profiles

$U1 < U2 < U3 < U4 < U5 < U6$
$U4 < U_{mf} < U5$

b)

Bed average voidage vs gas velocity

Fig. 4 Methods used for the determination of ε and ε_{mf}.

idization velocity, the axial pressure profiles converge at the same height, i.e. the aerated fixed bed height. For gas velocities higher than the minimum fluidization velocity, the axial pressure profiles are parallels and lead to heights increasing with gas velocity. Thus, for a given weight of olivine particles, the average bed voidage is calculated as below:

$$\varepsilon = 1 - \frac{m_P}{A_c \cdot H \cdot \rho_P} \qquad (8)$$

where ε, m_p, A_c, H and ρ_P are the bed average voidage, the solids inventory (kg), the cross-section of the gasifier (m²), the dense fluidized bed height (m) and the particle density (kg·m⁻³), respectively.

Regarding the minimum fluidization voidage, it is calculated using the bed height at minimum fluidization velocity (i.e. the aerated fixed bed height) and Equation 8. It is also determined from the method recommended by Botterill et al. (1982c) and Lucas et al. (1986). This method consists in plotting the bed average voidage, calculated through Equation 9, against the superficial gas velocity, and calculating the minimum fluidization voidage by extrapolating the results for $U = U_{mf}$. A typical example is illustrated in **Fig. 4b**. The blackened part of the curve, for gas velocities under the minimum fluidization velocity,

beds, the pressure standard deviation is zero. It only starts increasing with gas velocity when the bed is fluidized. Thus, the minimum fluidization velocity is considered as the intersection of the growing part of the curve and the gas velocities' axis.

These methods lead to similar results, with a relative error always under 10 %.

From the experimental results, the bed average voidage and minimum fluidization voidage can also be calculated. The bed average voidage is obtained by measuring and plotting the axial pressure profiles at several gas velocities (**Fig. 4a**). For gas velocities lower than the minimum flu-
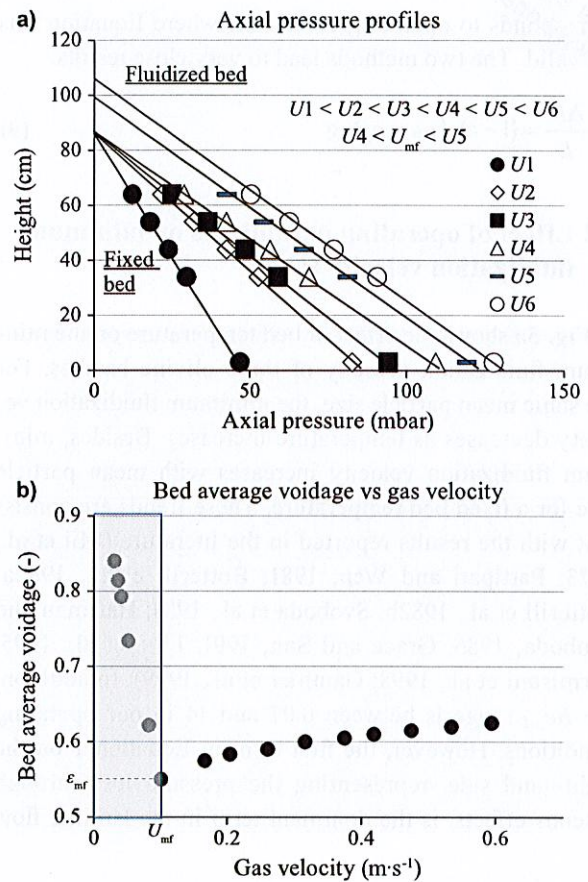
corresponds to operating conditions where Equation 9 is not valid. The two methods lead to very close results.

$$\frac{\Delta P}{L} = (1 - \varepsilon) \cdot (\rho_P - \rho_g) \cdot g \qquad (9)$$

3.2 Effect of operating parameters on minimum fluidization velocity (U_{mf})

Fig. 5a shows the effect of bed temperature on the minimum fluidization velocity of three olivine batches. For the same mean particle size, the minimum fluidization velocity decreases as temperature increases. Besides, minimum fluidization velocity increases with mean particle size for a fixed bed temperature. These trends are consistent with the results reported in the literature (Mii et al., 1973; Pattipati and Wen, 1981; Botterill et al., 1982a; Botterill et al., 1982b; Svoboda et al., 1983; Hartman and Svoboda, 1986; Grace and Sun, 1991; Llop et al., 1995; Formisani et al., 1998; Gauthier et al., 1999). In addition, the Re_{mf} range is between 0.07 and 14 in our operating conditions. However, the first term in Equation 1 on the right-hand side, representing the pressure loss through viscous effects, is the dominant term in the laminar flow

region ($Re < 10$). This indicates that Equation 1 can be rearranged to Equation 10.

$$Re < 10 \quad U_{mf} = \frac{d_p^2 \cdot \varphi^2}{150} \cdot \left(\frac{\rho_P - \rho_f}{\mu_f} \right) \cdot g \cdot \frac{\varepsilon_{mf}^3}{(1 - \varepsilon_{mf})} \qquad (10)$$

This equation shows that for fine particles, the viscous drag force (related to gas viscosity) has a major effect on the minimum fluidization velocity. Thus, an increase in gas viscosity with bed temperature leads to a rise in the viscous drag force which decreases the minimum fluidization velocity. Similarly, Equation 10 also shows that an increase in particle size yields a higher minimum fluidization velocity.

The nature of fluidizing gas (air or steam) also has an effect on the minimum fluidization velocity. **Fig. 5b** shows that the minimum fluidization velocity obtained with steam is higher than that obtained with air. These results are mainly explained by the low value of steam viscosity compared to air. The low value of steam density is also responsible for these trends. Values of density and viscosity for the two fluids are reported in **Table 5**.

Experimental results determined from about 40 tests carried out in the gasifier and in the combustor were compared to values predicted by 15 correlations of literature, given in **Table 1**. This comparison was based on the following statistical criteria, already defined in the work of Tannous et al. (1994):

- Relative error R_1:

$$R_1 = 100 \cdot \frac{1}{N_e} \cdot \sum_1^{N_e} \frac{Z_{exp} - Z_{predict}}{Z_{exp}} \qquad (11)$$

- Absolute relative error R_2:

$$R_2 = 100 \cdot \frac{1}{N_e} \cdot \sum_1^{N_e} \frac{|Z_{exp} - Z_{predict}|}{Z_{exp}} \qquad (12)$$

where Z_{exp} is the experimental value, $Z_{predict}$ is the predicted value and N_e is the number of experimental results compared to predictions. Values of R_1 and R_2 are given in **Table 6**. It was found that the relationships proposed by Bourgeois and Grenier (1968), Richardson (1971), Thonglimp et al. (1984) and Nakamura et al. (1985) represent our results with an absolute relative error similar to the experimental uncertainty (lower than 10 %). The best one is the correlation of Bourgeois and Grenier (1968)
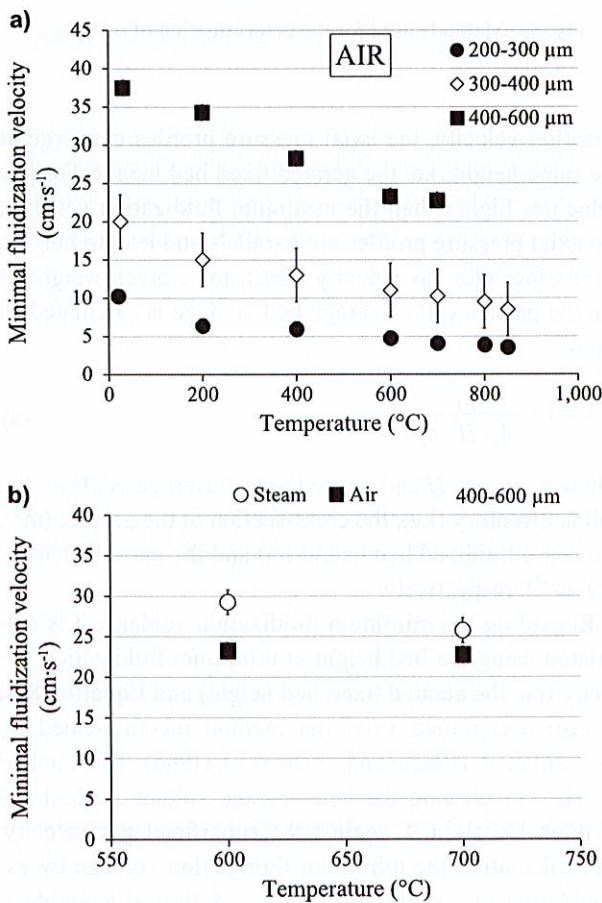
a)

b)

Fig. 5 Bed temperature effect on U_{mf} for different olivine batches (**a**) and for two fluidizing gases (**b**).

Table 5 Values of density and viscosity for steam and air at 600 and 700 °C.

Steam/Air	600 °C		700 °C	
Density (kg·m⁻³)	0.25	0.40	0.22	0.36
Viscosity (Pa·s)	3.41×10^{-5}	4.04×10^{-5}	3.85×10^{-5}	4.31×10^{-5}

Table 6 Prediction of minimum fluidization velocity: comparison between experimental findings and literature correlations.

Authors	R_1	R_2
Tannous et al. (1994)	–13 %	14 %
Wen and Yu (1966)	17 %	17 %
Bourgeois and Grenier (1968)	–3 %	8 %
Richardson (1971)	3 %	9 %
Saxena and Vogel (1977)	–51 %	51 %
Babu et al. (1978)	–71 %	72 %
McKay and McLain (1980)	–23 %	25 %
Svoboda et al. (1983)	–134 %	134 %
Chitester et al. (1984)	–17 %	18 %
Thonglimp et al. (1984)	8 %	10 %
Nakamura et al. (1985)	6 %	9 %
Lucas et al. (1986)	17 %	17 %
Chyang and Huang (1988)	31 %	31 %
Murachman (1990)	–14 %	17 %
Fatah (1991)	–6 %	36 %

with a relative error equal to –3 %.

A new correlation is proposed (Equation 13) in order to estimate the minimum fluidization velocity of olivine particles as a function of bed temperature, particle size and fluidizing gas nature. This correlation was established between 20 and 950 °C, with olivine particles of mean Sauter diameter between 282 and 689 μm and for air and steam as fluidizing gas. It is intended to be used for the design of FICFB biomass gasifiers operating with olivine as the heat transfer medium.

$$Re_{mf} = (20.32^2 + 0.031 \cdot Ar)^{0.5} - 20.32 \qquad (13)$$

This correlation enables prediction of experimental U_{mf} with a relative error R_1 equal to –2 % and an absolute relative error of 8 % (Fig. 6).

3.3 Effect of operating parameters on bed voidage

Fig. 7 shows that bed voidage at minimum fluidization conditions (ε_{mf}) is independent of bed temperature and mean particle size. The estimated bed voidage is about 0.55, which is slightly higher than the mean voidage of an aerated fixed bed ε_{BA}. Tests carried out in the combustor between 700 and 950 °C lead to the same conclusions. These results are likely explained by the fact that for class-B particles, the absence of interparticle force leads to an almost instantaneous transition between fixed bed and fluidized bed states (no deaeration phenomenon).
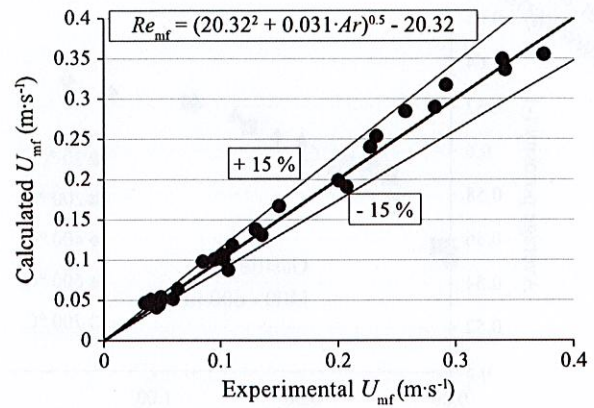
Fig. 6 Prediction of minimum fluidization velocity: comparison between experimental findings and proposed correlation.
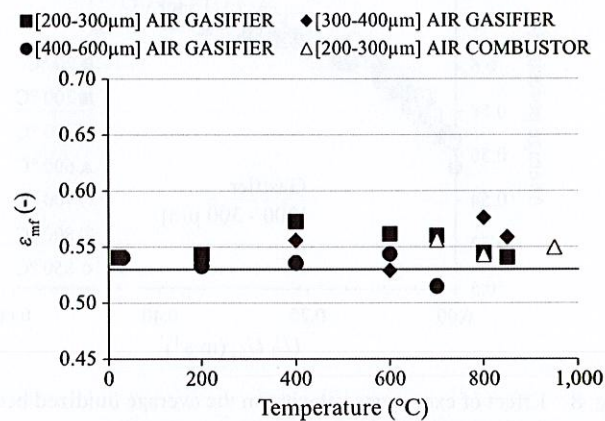
Fig. 7 Effect of bed temperature on minimum fluidization voidage for different olivine batches.

Thus, for this class of particles, minimum fluidization voidage is almost equal to the fixed bed voidage.

Fig. 8a, Fig. 8b and Fig. 8c show the average bed voidage evolution vs excess gas velocity ($U-U_{mf}$), at different bed temperatures (between 20 °C and 850 °C), for 3 olivine batches. The average bed voidage increases with excess gas velocity, regardless of particle size and bed temperature. Besides, for the same excess gas velocity, bed voidage is slightly affected by bed temperature and particle size. Tests carried out in the combustor between 700 and 950 °C confirm these results (Fig. 8d). These trends are consistent with the experimental findings reported in the literature (Botterill et al., 1982a; Botterill et al., 1982c). They may be related to the fact that bed expansion is mainly caused by the presence of bubbles in the bed. Bed voidage can be estimated from Equation 14 (Kunii and Levenspiel, 1991), which strongly depends on bubble properties:

$$\varepsilon = \delta_B + (1 - \delta_B) \cdot \varepsilon_{mf} \qquad (14)$$
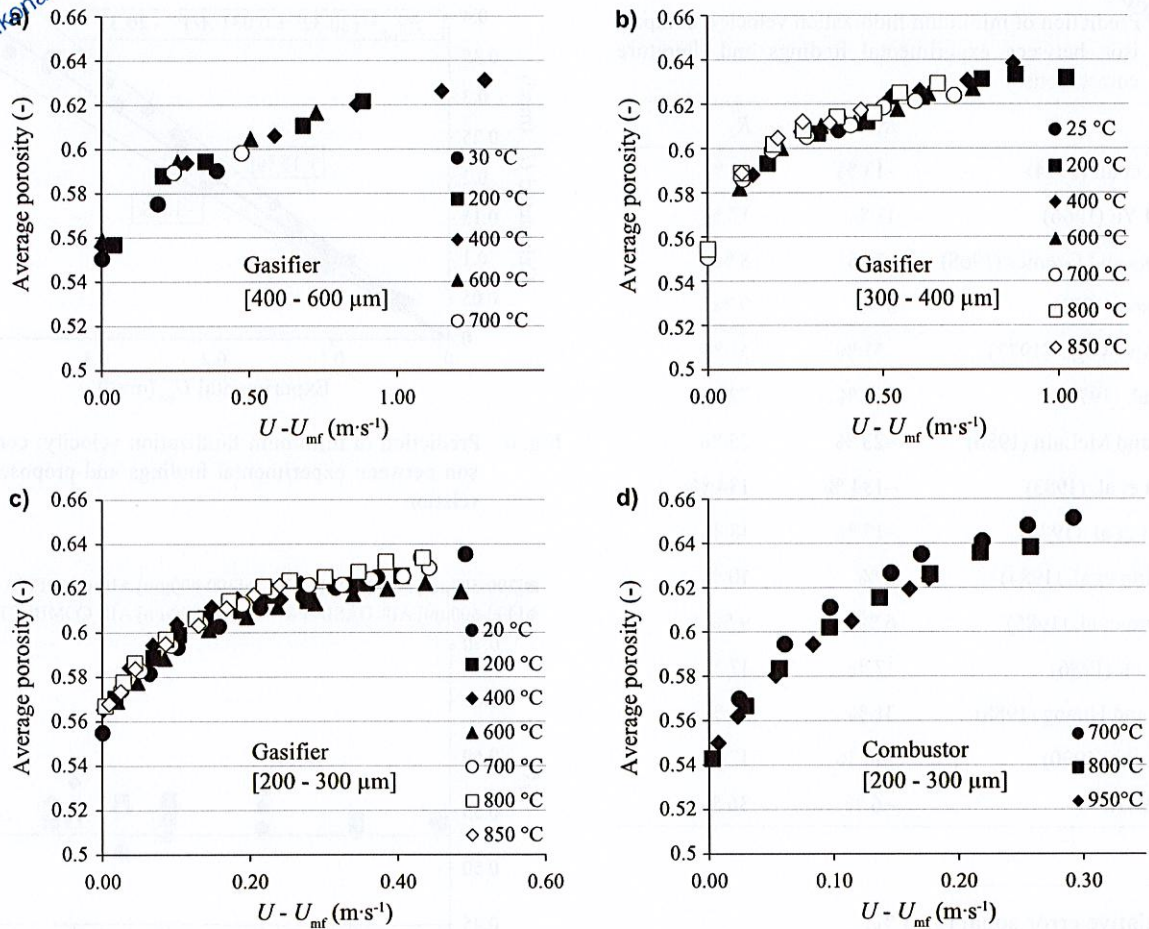
In Equation 14, the bubble volume fraction in the bed

Fig. 8 Effect of excess gas velocity on the average fluidized bed voidage, for different bed temperatures and olivine batches in the gasifier (**a**, **b**, **c**) and the combustor (**d**).

δ_B mainly depends on excess gas velocity U-U_{mf}, as described in **Appendix A**. Thus, average bed voidage depends only on excess gas velocity, as observed in our experiments.

Experimental ε values determined from about forty tests in both gasifier and combustor were compared to values predicted from literature correlations, reported in **Table 2**. These correlations are usually used for fluidized bed reactor design, modeling and simulation. Relative error R_1 and absolute relative error R_2 were calculated and are presented in **Table 7**. For our operating conditions and olivine particles, the relationships proposed by Lewis et al. (1949), Matsen et al. (1969), and Thonglimp et al. (1984) are the most adapted. The best one is the correlation of Matsen et al. (1969) with a relative error of −10 % and an absolute relative error of 10 % (**Fig. 9**).

A new correlation (Equation 15) that takes into account fluidized bed temperature, mean particle size and fluidizing gas nature is proposed in order to estimate the average bed voidage of a bubbling fluidized bed of olivine particles. This correlation was established between 20 and 950 °C, with olivine particles of mean Sauter diameter between 282 and 689 μm and for air and steam as fluidiz-

Table 7 Prediction of average bed voidage: comparison between experimental findings and literature correlations.

Authors	R_1	R_2
Thonglimp et al. (1984)	10 %	13 %
Chyang and Huang (1988)	30 %	30 %
Lewis et al. (1949)	−11 %	11 %
Matsen et al. (1969)	−10 %	10 %
Hilal and Gunn (2002)	−20 %	20 %

ing gas. It is intended to be used for the design of FICFB biomass gasifiers which operate with olivine as the heat transfer medium.

$$\frac{\varepsilon}{\varepsilon_{mf}} = 1.0394 \cdot \left(\frac{U - U_{mf}}{U_{mf}}\right)^{0.026} \cdot Ar^{0.006} \tag{15}$$

This correlation enables the prediction of experimental ε with a relative error and an absolute relative error both equal to 1 % (**Fig. 10**). It is interesting to notice that despite the low coefficient applied to the Archimedes number, its contribution cannot be ignored. Indeed, for some
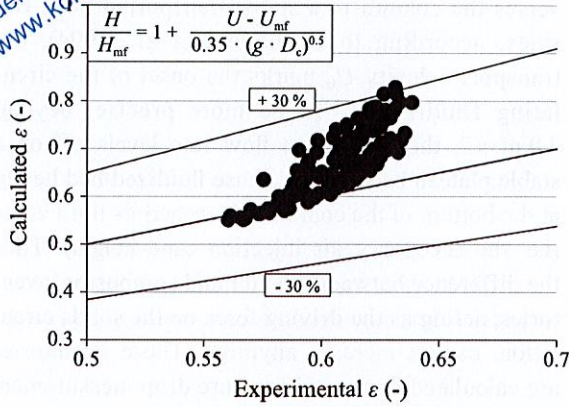
$$\frac{H}{H_{mf}} = 1 + \frac{U - U_{mf}}{0.35 \cdot (g \cdot D_c)^{0.5}}$$

Fig. 9 Comparison between ε experimental findings and predictions of the Matsen et al. (1969) correlation.

$$\frac{\varepsilon}{\varepsilon_{mf}} = 1.0394 \cdot \left(\frac{U - U_{mf}}{U_{mf}}\right)^{0.026} \cdot Ar^{0.006}$$
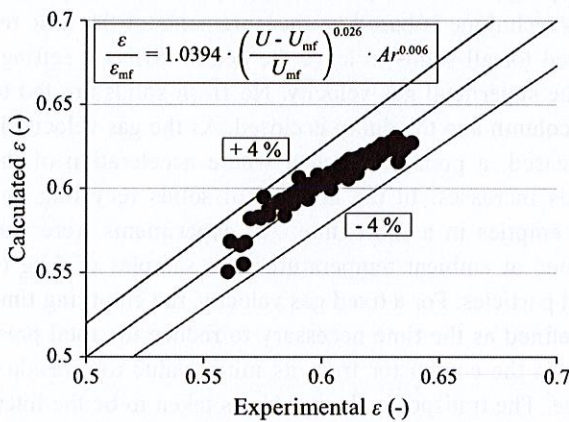
Fig. 10 Prediction of average bed voidage: Comparison between experimental findings and proposed correlation.

experiments ($T = 30\,°C$ and $d_p = $ [400–600 μm]), the Archimedes number is almost equal to 25,000. In these cases, the Archimedes number contribution is about 6 %.

4. Circulating fluidized bed hydrodynamic study

The biomass gasification efficiency in an FICFB mainly depends on heat transfer medium circulation flow rate. Thus, it appears essential to identify the key parameters influencing the circulation flow rate.

Process parameters are: gas velocity in the gasifier U_G, gas velocity in the standpipe U_S, particle inventory m_p, bed temperature T, secondary air injection position H_{II} and air average velocity in the combustor U_{comb}. The last parameter depends on primary and secondary air flow rates in the combustor. However, in order to ensure a good fluidization in the dense fluidized bed of the combustor, the primary air flow rate is set so that $U_I = 4 \cdot U_{mf}(T)$. Based on previous work (Detournay, 2011), the value of

Table 8 Operating conditions of circulation experiments.

	Reference	Range
m_p (kg)	35	35–60
U_G (U/U_{mf})	4	1–8
U_{comb} (U/U_t)	2.4	0.5–3
H_{II} (cm)	15	15
U_S (U/U_{mf})	8	1–9
T (°C)	500	20–850

Table 9 Effect of bed temperature on terminal settling velocity of single olivine and sand particles.

Temperature (°C)	20	300	500	800	850
U_t (m·s⁻¹)–Olivine	2.05	2.10	2.03	1.90	1.88
U_t (m·s⁻¹)–Sand	1.92	1.91	1.81	1.67	1.65

the secondary air injection position (injection cane height H_{II}) is set at 15 cm. Thus, only the secondary air flow rate, called "transport air", is varied in our experiments. For each experiment, temperatures in both gasifier and combustor were set at almost identical values.

Most of the experiments were performed with the olivine batch [200–300 μm] as bed material, between 20 and 850 °C. However, some tests were also carried out with sand particles at ambient temperature, in order to investigate the effect of the bed material nature. The properties of these materials are reported in **Table 4**.

Table 8 indicates the variation range of the process parameters in this study. In this table, U_t is the terminal settling velocity of the particles used. It is given by:

$$U_t = \left[\frac{4 \cdot d_p \cdot (\rho_P - \rho_g) \cdot g}{3 \cdot C_d \cdot \rho_g}\right]^{1/2} \quad (16)$$

where C_d is the drag coefficient. The latter depends on the solids shape factor φ, and is estimated by (Haider and Levenspiel, 1989):

$$C_d = \frac{24}{Re_t} \cdot \left[1 + 8.17 \cdot e^{-4.0655 \cdot \varphi} \cdot Re_t^{(0.0964 + 0.5565 \cdot \varphi)}\right.$$

$$\left. + \frac{73.69 \cdot e^{-5.0748 \cdot \varphi} \cdot Re_t}{Re_t + 5.378 \cdot e^{6.2122 \cdot \varphi}}\right] \quad (17)$$

where Re_t is the Reynolds number at $U = U_t$.

Besides, in **Table 9**, the values of U_t calculated for several temperatures between 20 and 850 °C are reported for both sand and olivine particles. It can be noticed that olivine and sand particles have close values of U_t, in particular at ambient temperature. Besides, U_t velocity only decreases by 8 and 13 % between 20 and 850 °C, for olivine

and sand particles, respectively.

A previous study (Detournay, 2011) carried out at ambient temperature on the same pilot as the one used in this work showed that:

- Gas flow rate in both gasifier and standpipe do not have any effect on the solids circulation flow rate for gas velocities higher than 1.5 times the minimum fluidization velocity;
- key parameters are U_{comb} and solids inventory m_p.

Experiments carried out in this study for temperatures up to 850 °C confirm these trends.

4.1 Determination of transport velocity: Presentation of a typical example

Fig. 11 presents a typical example regarding the effect of gas velocity on solids circulation flow rate, using sand as bed material. Three regimes can be observed:

- For gas velocities lower than U_t (1.9 m·s^{-1}): a very low solids circulation flow rate is measured (about 10–20 kg·h^{-1}). For these velocities, the combustor is a deep «dense fluidized bed», whose height can exceed 1 m. Thus, elutriation of the fine particles initially present in the solids batch explains the residual values of circulation flow rate;
- for gas velocities between 1.9 and 3.3 m·s^{-1}: a transitional regime is observed. Circulation mass flow rate is found to increase from 30 to 200 kg·h^{-1}. This is likely attributed to the fact that the kinetic energy contained in the bubbles during their eruption at the bed surface is enough to transport particles brought into its wake to the combustor outlet;
- for gas velocities higher than 3.3 m·s^{-1} (= 1.6 · U_t): the solids mass flow rate sharply increases before reaching a plateau. According to the definition proposed by Yerushalmi and Cankurt (1979), this velocity is the transport velocity U_{tr} at which the solids tra-

verses the column in a stable transported flow. Besides, according to Chehbouni et al. (1994), the transport velocity U_{tr} marks the onset of the circulating fluidization. To be more precise, beyond 4.0 m·s^{-1}, the circulation flow rate levels off on a stable plateau because the dense fluidized bed height at the bottom of the combustor reached its limit value (i.e. the secondary air injection cane height). Thus the difference between gasifier and combustor inventories, acting as the driving force on the solids circulation, cannot increase anymore. These inventories are calculated from total pressure drop measurement in gasifier and combustor.

In order to ascertain the appropriateness of the U_{tr} value measured in this study and presented above, the emptying time technique was employed (Han et al., 1985). This technique is based on measurements of the time required for all solids to leave the bed at different settings of the superficial gas velocity. No fresh solids are fed to the column and the dump is closed. As the gas velocity is increased, a point is reached where acceleration of the solids increases. In the absence of solids recycling, the bed empties in a short time. All experiments were performed at ambient temperature with samples of 7 kg of sand particles. For a fixed gas velocity, the emptying time is defined as the time necessary to reduce the total pressure in the combustor from its initial value to a residual value. The transport velocity, U_{tr}, is taken to be the intersection of the lines of low and high accelerations (**Fig. 12**). The value of U_{tr} measured by this method is 3.4 m·s^{-1}, which is consistent with the value obtained from **Fig. 11** (i.e. 3.3 m·s^{-1}).

In order to investigate the effect of the bed material nature on solids circulation, the results previously obtained with sand particles were compared with new ones obtained using olivine particles, for a bed material inventory of 35 kg (**Fig. 13**). It was found that the solids mass flow rate evolution vs gas velocity is not significantly affected
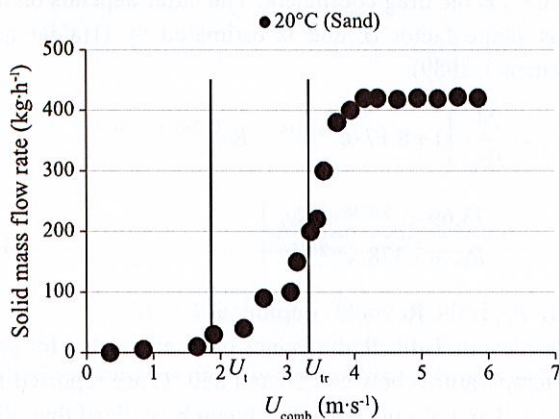
Fig. 11 Effect of combustor gas velocity on circulating solids mass flow rate (sand, $m_p = 35$ kg, $U_G = 4 \cdot U_{mf}$, $U_I = 4 \cdot U_{mf}$, $H_{II} = 15$ cm).
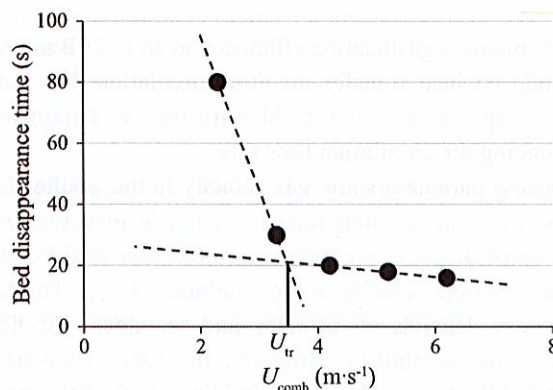
Fig. 12 Effect of combustor gas velocity on the disappearance time of solids (sand, $m_p = 7$ kg, $T = 20$ °C).
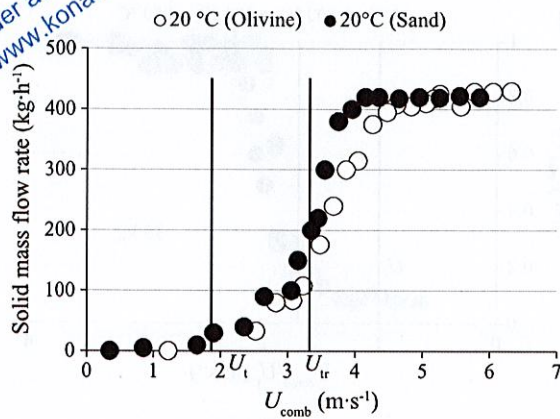
Fig. 13 Effect of bed material nature on circulating solids mass flow rate ($U_G = 4 \cdot U_{mf}$, $U_I = 4 \cdot U_{mf}$, $m_p = 35$ kg, $H_{II} = 15$ cm).

by the bed material nature when solids batches have similar U_t values. Results show that the same transport velocity U_{tr} and circulation mass flow rate on the plateau were found with olivine particles regarding the values obtained with sand.

According to Perales et al. (1991a), the transport velocity is directly proportional to the terminal settling velocity with a ratio between U_{tr} and U_t equal to 1.7. This value is close to the one presented above. Besides, **Fig. 14a** shows that for an increase in combustor gas velocity U_{comb}, the gasifier inventory increases almost linearly before reaching a plateau.

Regarding combustor inventory, it decreases as gas velocity rises, and also reaches a plateau. Thus, results show that **the difference between gasifier and combustor inventories presented in Fig. 14b increases with combustor gas velocity before levelling off. This trend is similar to the one of solids mass flow rate vs. gas velocity.**

This is consistent since the difference between gasifier and combustor inventories is directly related to the difference in pressures between these two reactors. However, the latter acts as the driving force on solids circulation. Thus a rise in combustor gas velocity produces an increase in pressure difference between gasifier and combustor, leading to higher solids circulation flow rates. These trends are consistent with the ones presented above for sand particles.

4.2 Effect of bed material inventory and temperature

Fig. 15 presents the effect of the bed material inventory, between 20 and 60 kg, on the solids circulation flow rate for a given combustor air velocity ($U_{comb} = 3.6$ m·s^{-1}), with sand particles as the bed material. Results show that a rise in bed material inventory leads to higher solids mass flow rates. Besides, **Fig. 16** presents the effect of
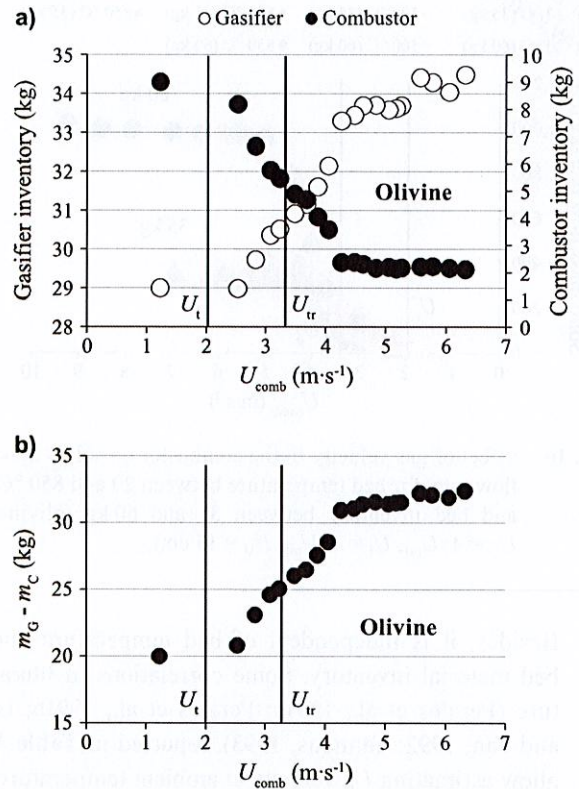

Fig. 14 Effect of gas velocity in the combustor on gasifier and combustor inventories (olivine, $U_G = 4 \cdot U_{mf}$, $U_I = 4 \cdot U_{mf}$, $m_p = 35$ kg, $H_{II} = 15$ cm).
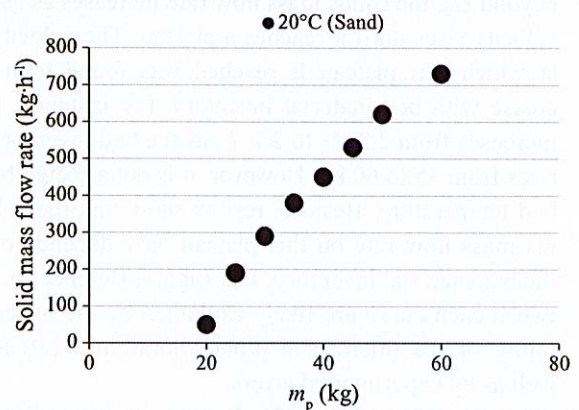

Fig. 15 Effect of bed material inventory on circulating solids mass flow rate (sand, $T = 20$ °C, $U_G = 4 \cdot U_{mf}$, $U_I = 4 \cdot U_{mf}$, $U_{II} = 3.3$ m·s^{-1}, $H_{II} = 15$ cm).

bed temperature, between 20 and 850 °C, on olivine circulation flow rate vs. combustor gas velocity, for 35- and 60-kg bed inventories. It can be noticed that for each bed temperature and bed material inventory, the curves follow the same trends. Besides, results show that:

- For gas velocities lower than U_{tr}, the solids mass flow rate is not affected by the bed temperature or inventory;
- the solids circulation onset, at $U = U_{tr}$, was found to be reached for a gas velocity between 1.6 and $1.7 \cdot U_t$
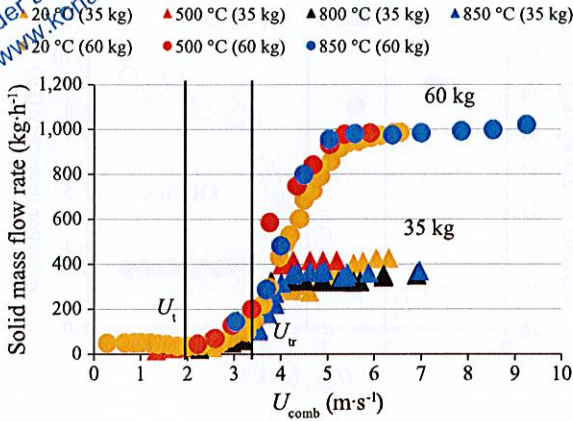
Fig. 16 Effect of gas velocity in the combustor on solids mass flow rate, for bed temperature between 20 and 850 °C, and bed inventory between 35 and 60 kg (olivine, $U_G = 4 \cdot U_{mf}$, $U_I = 4 \cdot U_{mf}$, $H_{II} = 15$ cm).

Besides, it is independent of bed temperature and bed material inventory. Some correlations in literature (Perales et al., 1991a; Perales et al., 1991b; Bi and Fan, 1992; Tannous, 1993), reported in **Table 3**, allow estimating U_{tr} velocity at ambient temperature, with relative errors between –6 and 2 %. However, for bed temperatures higher than ambient temperature, only the correlation proposed by Perales et al. (1991a) properly estimates U_{tr} values;

- beyond U_{tr}, the solids mass flow rate increases as gas velocity rises until it reaches a plateau. The velocity at which this plateau is reached was found to increase with bed material inventory. For instance, it **increases from $2.2 \cdot U_t$ to $2.7 \cdot U_t$ as the bed inventory rises from 35 to 60 kg. However, it is not affected by bed temperature.** Besides, results show that the solids mass flow rate on this plateau only depends on the bed material inventory. The slight differences between each curve are likely explained by the uncertainty of the microwave probe (SolidFlow 2.0) as well as by experimental errors.

Besides, **Fig. 17a** and **Fig. 17b** illustrate the normalized solids mass flow rate (Fp/Fp_{max}) vs. the normalized gas velocity (U_{comb}/U_t), between 20 and 850 °C, for bed inventories of 35 and 60 kg, respectively. Results confirm that U_{tr} velocity is not affected by bed temperature or bed inventory.

4.3 Comments on the effect of combustor gas velocity on solids mass flow rate and total pressure drop fluctuations

An experiment was carried out at 500 °C for an olivine inventory of 35 kg. **Fig. 18** shows the influence of combustor air velocity U_{comb} on the normalized circulating solids mass flow rate Fp/Fp_{max}, total pressure in the com-
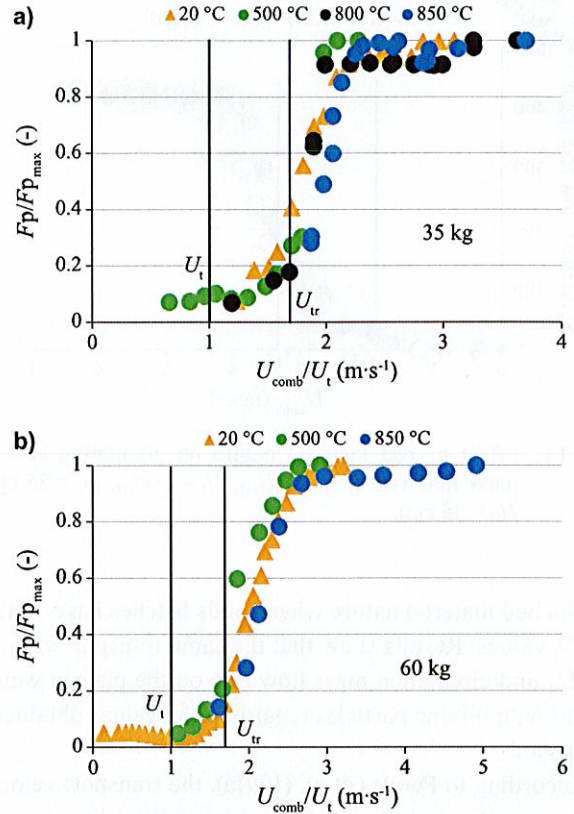

Fig. 17 Effect of bed temperature on normalized solids flow rate vs. normalized gas velocity for 35 **(a)** and 60 **(b)** bed material inventories (olivine, $U_G = 4 \cdot U_{mf}$, $U_I = 4 \cdot U_{mf}$, $H_{II} = 15$ cm).

bustor P_{comb}, pressure profiles along the combustor and distribution of solids inventory in both gasifier and combustor. Total pressure is considered as the pressure difference between two pressure taps, P_{dist} (**3 cm above the distributor**) and P_7 (2.5 m above the distributor). From the **temporal fluctuations of solids flow rate and total pressure** in the combustor, a standard deviation was determined for several velocities U_{comb}. Results show that the hydrodynamic regimes defined above, as well as the transport velocity, can be estimated from the plot of these standard deviations against gas velocity. For instance, it was found from results at 500 °C that:

- For velocities up to 2.4 m·s^{-1} (zone 1 in **Fig. 18**), solids inventories in both gasifier and combustor remain almost constant, which is in agreement with the constant total pressure of the combustor. Moreover, a very low solids circulation flow rate is measured. As mentioned above, the combustor is a deep «dense fluidized bed» with a height reaching 1.5 m (**Fig. 18c**). In this zone, the solids concentration in the free-board area is very small. Thus elutriation of fine particles initially present in the solids batch explains the residual values of the circulation flow rate. Besides, an increase in gas velocity leads to a peak in the combustor pressure standard deviation
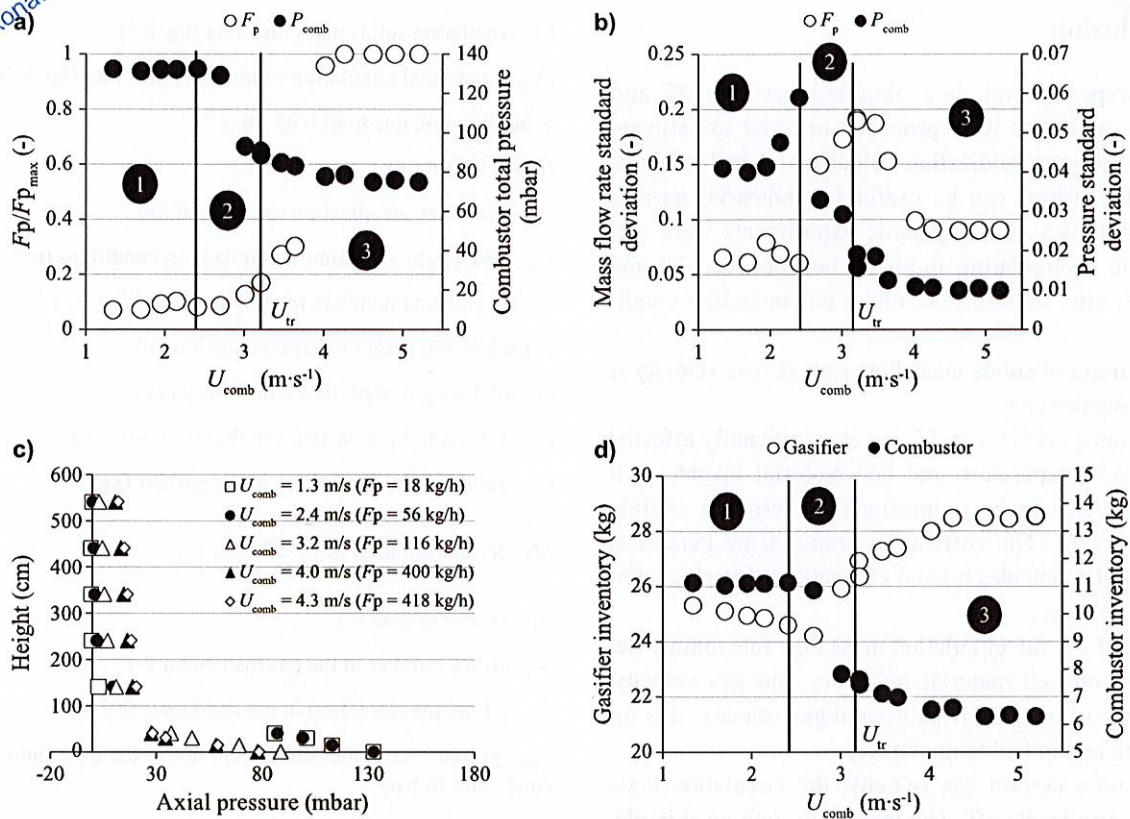
Fig. 18 Effect of combustor gas velocity on the solids mass flow rate, the combustor total pressure (a), its standard deviation (b), the axial pressure profiles (c) as well as on solids inventory in both gasifier and combustor (d) (olivine, $m_p = 35$ kg, $T = 500$ °C).

(Fig. 18b). According to many authors (Yerushalmi and Cankurt, 1979; Han et al., 1985; Mori et al., 1986; Chehbouni et al., 1994), this peak is explained by the slugging phenomenon due to an increase in bubble formation and coalescence. These authors defined this velocity as the onset of turbulent fluidization, U_c. It can be noticed that this velocity is slightly higher than the terminal settling velocity U_t (2.03 m·s^{-1} at 500 °C);

- for velocities between 2.4 and 3.2 m·s^{-1} (zone 2), an increase in the circulation mass flow rate from 50 to 120 kg·h^{-1} and an abrupt rise of its standard deviation are observed. As explained above, this is likely attributed to the fact that the kinetic energy contained in the bubbles during their eruption at the bed surface is enough to transport particles brought into its wake to the combustor outlet. This phenomenon, as shown in **Fig. 18d**, leads to an increase in the inventory difference between both reactors (i.e. the pressure difference on both sides of the dump). Consequently, a decrease in the total pressure of the combustor was observed (**Fig. 18a**). The total pressure standard deviation was also found to decrease (**Fig. 18b**). Some authors (Yerushalmi and Cankurt, 1979; Han et al., 1985; Satija and Fan, 1985; Mori et

al., 1986; Perales et al., 1991a; Tannous, 1993) explain this trend by the breakup of bubbles and slugs due to internal solids circulation, and by the decrease in bubble formation and coalescence;

- for velocities beyond 3.2 m·s^{-1} (zone 3), the solids mass flow rate increases before reaching a plateau. Simultaneously, its standard deviation decreases to a stable stage. According to Chehbouni et al. (1994), these trends indicate that the velocity at which this third zone starts is the transport velocity, U_{tr}, which marks the onset of the circulating fluidization. Worthy of note is that the value of U_{tr} found from the evolution of solids mass flow rate standard deviation vs. gas velocity is close to the one determined above (3.3 m·s^{-1}). For velocities higher than 4.0 m·s^{-1}, the stabilization of the solids mass flow rate, combustor total pressure and inventory difference between both reactors is in agreement with the results of **Yerushalmi and Cankurt (1979)**. These authors found that beyond the transport velocity U_{tr}, solid traverses the column in a stable transported flow.

However, supplementary studies have to be performed in order to ascertain the good reproducibility of circulation flow rate and total pressure standard deviation.

5. Conclusion

From experimental data obtained between 20 and 950 °C, correlations were proposed in order to estimate olivine minimum fluidization velocity and bed voidage. These relationships can be useful for industrial gasifier design. Moreover, hydrodynamic experiments were carried out in a circulating fluidized bed between 20 and 850 °C. Results showed that, under our operating conditions:

- The trend of solids mass flow rate vs. gas velocity is of S-shape type;
- the transport velocity U_{tr} is not significantly affected by bed temperature and bed material inventory. It only seems to be proportional to terminal settling velocity U_t. The correlation proposed by Perales et al. (1991a) enables a good estimate of this characteristic velocity;
- beyond U_{tr}, the circulation mass flow rate mainly depends on bed material inventory and gas velocity. For the same bed inventory and gas velocity, it is independent of bed temperature;
- beyond a certain gas velocity, the circulation mass flow rate levels off. The mass flow rate on this plateau is not affected by bed temperature but is strongly dependent on bed material inventory.

Besides, results showed that key parameters for the solids flow rate control are combustor gas velocity and solids inventory. An increase in these parameters leads to higher circulation flow rates. However, the bed temperature and bed material nature showed no influence, neither on the transport velocity nor on the solids flow rate.

Nomenclature

A_c: reactor section (m²)

Ar: Archimedes number (–)

C_1, C_2: constant numbers relating to Ar and Re_{mf} (–)

C_{11}: constant number, $C_{11} = 0.64 \cdot A_c^{0.4}$ (m$^{0.8}$)

C_{12}: constant number, $C_{12} = \dfrac{1.30}{g^{0.2} \cdot N_{or}^{0.4}}$ (m$^{-0.2} \cdot$ s$^{0.4}$)

C_d: drag coefficient (–)

C_v: diameter variation coefficient (–)

$\overline{d_B}$: bubble mean diameter (m)

d_{B0}: initial bubble diameter, at the outlet of the gas distributor (m)

d_{Bm}: maximal bubble diameter (m)

d_p: Sauter mean particle diameter (m)

D_C: reactor diameter (m)

Fp: circulating solids mass flow rate (kg·h^{-1})

Fp_{max}: maximal circulating solids mass flow rate (kg·h^{-1})

g: acceleration due to gravity (m·s^{-2})

H: bed height (m)

H_{II}: secondary air injection cane height (m)

H_{mf}: bed height at minimum fluidization conditions (m)

K_1, K_2: constant numbers relating to Ar and Re_{mf} (–)

L: packed bed height in Ergun equation (m)

m_p: total weight of particles, inventory (kg)

m_{pC}: total weight of particles in the combustor (kg)

m_{pG}: total weight of particles in the gasifier (kg)

Mv: density number, $Mv = \dfrac{\rho_P - \rho_f}{\rho_f}$ (–)

N_e: number of data (–)

N_{or}: orifice number in the gas distributor (–)

P_{comb}: total pressure drop in the combustor (mbar)

P_{dist}: pressure drop measured 3 cm above the distributor, in the combustor (mbar)

R_1: relative error (%)

R_2: absolute relative error (%)

Re_{mf}: Reynolds number at the minimum fluidization point (–)

Re_{tr}: Reynolds number at the gas velocity U_{tr} (–)

T: temperature (°C)

U: superficial gas velocity (m·s^{-1})

U_b: bubble rise velocity in the bed (m·s^{-1})

U_c: turbulent regime characteristic velocity (m·s^{-1})

U_{ch}: chocking velocity (m·s^{-1})

U_{comb}: total air velocity in the combustor (m·s^{-1})

U_G: gas velocity in the gasifier (m·s^{-1})

U_I: primary air velocity in the combustor (m·s^{-1})

U_{II}: secondary air velocity in the combustor (m·s^{-1})

U_{mf}: minimum fluidization velocity (m·s^{-1})

U_s: superficial gas velocity in the standpipe (m·s^{-1})

U_t: terminal settling velocity of single particle (m·s^{-1})

U_{tr}: transport velocity (m·s^{-1})

z: given height in the dense fluidized bed (m)

$\overline{Z}$: mean value of a given parameter (unit of the parameter)

Z_i: value of a given parameter (unit of the parameter)

Greek symbols

γ: compressibility factor (–)

δ_B: bubble volume fraction in the bed (–)

ΔP: pressure drop (Pa)

ε: average fluidized bed voidage (–)

ε_{BA}: mean aerated bulk bed voidage (–)

ε_{BP}: mean packed bulk bed voidage (–)

ε_{mf}: minimum fluidization voidage (–)

μ_f: fluid viscosity (kg·m^{-1}·s^{-1})

ρ_b: bed density (kg·m^{-3})

ρ_{BA}: aerated bulk density (kg·m^{-3})

ρ_{BP}: packed bulk density (kg·m^{-3})

ρ_f: fluid density (kg·m^{-3})

ρ_{mf}: bed density at the minimum fluidization condition (kg·m^{-3})

ρ_p: particle density (kg·m^{-3})

ρ_s: skeletal density (kg·m^{-3})

σ_Z: normalized standard deviation (–)

φ: shape (sphericity) factor (–)

χ: particle internal voidage (–)

References

Adanez J., De Diego L.F., Gayan P., Transport velocities of coal and sand particles, Powder Technology, 77 (1993) 61–68.

Agarwal O.P., Storrow J.A., Pressure drop in fluidization beds, Chemistry & Industry, 15 (1951) 278–286.

Babu S.P., Shah B., Talwalkar A., Fluidization correlations for coal gasification materials-minimum fluidization velocity and fluidized bed expansion ratio, AIChE Symposium Series, 74 (1978) 176–186.

Basu P., Cheng L., An analysis of loop seal operations in a circulating fluidized bed, Chemical Engineering Research and Design, 78 (2000) 991–998.

Berruti F., Pugsley T.S., Godfroy L., Chaouki J., Patience G.S., Hydrodynamics of circulating fluidized bed risers: a review, The Canadian Journal of Chemical Engineering, 73 (1995) 579–602.

Bi X., Fan L.-S., Existence of turbulent regime in gas-solid fluidization, AIChE journal, 38 (1992) 297–301.

Bi X., Grace J.R., Effects of pressure and temperature on flow regimes in gas-solid fluidization systems, The Canadian Journal of Chemical Engineering, 74 (1996) 1025–1027.

Botterill J.S.M., Teoman Y., Yuregir K.R., Comments on 'Minimum fluidization velocity at high temperature', Industrial & Engineering Chemistry Process Design and Development, 21 (1982a) 784–785.

Botterill J.S.M., Teoman Y., Yuregir K.R., The effect of operating temperature on the velocity of minimum fluidization, bed voidage and general behaviour, Powder Technology, 31 (1982b) 101–110.

Botterill J.S.M., Teoman Y., Yuregir K.R., The effect of temperature on fluidized bed behaviour, Chemical Engineering Communications, 15 (1982c) 227–238.

Bourgeois P., Grenier P., The ratio of terminal velocity to minimum fluidising velocity for spherical particles, The Canadian Journal of Chemical Engineering, 46 (1968) 325–328.

Bull D.R., Performance improvements to a fast internally circulating fluidised bed (FICFB) biomass gasifier for combined heat and power plants (Doctoral dissertation), University of Canterbury, 2008.

Cai P., Jin Y., Yu Z.-Q., Wang Z.-W., Mechanism of flow regime transition from bubbling to turbulent fluidization, AIChE journal, 36 (1990) 955–956.

Chehbouni A., Chaouki J., Guy C., Klvana D., Characterization of the flow transition between bubbling and turbulent fluidization, Industrial & Engineering Chemistry Research, 33 (1994) 1889–1896.

Chehbouni A., Chaouki J., Guy C., Klvana D., Effects of different parameters on the onset of fluidization in a turbulent regime, Canadian Journal of Chemical Engineering, 73 (1995) 41–50.

Chitester D., Kornosky R.M., Fan L.-S., Danko J.P., Characteristics of fluidization at high pressure, Chemical Engineering Science, 39 (1984) 253–261.

Chyang C.S., Huang W.C., Characteristics of large particle fluidization, Journal of The Chinese Institution of Chemical Engineers, 19 (1988) 81–89.

Davidson J.F., Harrison D., Fluidized Particles, Cambridge University Press, Cambridge, England, 1963.

Detournay M., Vapogazéification de la biomasse en Lit Fluidisé Circulant: Élaboration des outils théoriques et expérimentaux (Doctoral dissertation), Institut National Polytechnique de Toulouse, 2011.

Ergun S., Fluid flow through packed columns, Chemical Engineering Progress, 48 (1952) 89–94.

Fan L.T., Ho T.-C., Walawender W.P., Measurements of the rise velocities of bubbles, slugs and pressure waves in a gas-solid fluidized bed using pressure fluctuation signals, AIChE Journal, 29 (1983) 33–39.

Fatah N., Fluidisation des grosses particules à haute température hydrodynamique et transferts thermiques, Institut National Polytechnique de Toulouse, 1991.

Formisani B., Girimonte R., Mancuso L., Analysis of the fluidization process of particle beds at high temperature, Chemical Engineering Science, 53 (1998) 951–961.

Gauthier D., Zerguerras S., Flamant G., Influence of the particle size distribution of powders on the velocities of minimum and complete fluidization, Chemical Engineering Journal, 74 (1999) 181–196.

Geldart D., The effect of particle size and size distribution on the behaviour of gas-fluidised beds, Powder Technology, 6 (1972) 201–215.

Geldart D., Types of gas fluidization, Powder Technology, 7 (1973) 285–292.

Gómez-Barea A., Leckner B., Modeling of biomass gasification in fluidized bed, Progress in Energy and Combustion Science, 36 (2010) 444–509.

Goo J.H., Seo M.W., Kim S.D., Song B.H., Effects of temperature and particle size on minimum fluidization and transport velocities in a dual fluidized bed, Proceedings of the 20th International Conference on Fluidized Bed Combustion,

Xian, 2009, pp. 305–309.

Grace J.R., Sun G., Influence of particle size distribution on the performance of fluidized bed reactors, The Canadian Journal of Chemical Engineering, 69 (1991) 1126–1134.

Grace J.R., Knowlton T.M., Avidan A.A., Circulating Fluidized Beds, 1st ed., Blackie Academic and Professional, London, UK, 1997.

Haider A., Levenspiel O., Drag coefficient and terminal velocity of spherical and nonspherical particles, Powder Technology, 58 (1989) 63–70.

Han G.Y., Lee G.S., Kim S.D., Hydrodynamic characteristics of a circulating fluidized bed, Korean Journal of Chemical Engineering, 2 (1985) 141–147.

Hartman M., Svoboda K., Predicting the effect of operating temperature on the minimum fluidization velocity, Industrial & Engineering Chemistry Process Design and Development, 25 (1986) 649–654.

Hilal N., Gunn D.J., Solid hold up in gas fluidised beds, Chemical Engineering and Processing: Process Intensification, 41 (2002) 373–379.

Hofbauer H., Rauch R., Löffler G., Kaiser S., Fercher E., Tremmel H., Six years of experience with the FICFB-gasification process, In: 12th European conference on biomass and bioenergy. Amsterdam, The Netherlands, 2002.

Kunii D., Levenspiel O., Fluidization Engineering, 2nd ed., Butterworth-Heinemann, Stoneham, USA, 1991.

Lee G.S., Kim S.D., Bed expansion characteristics and transition velocity in turbulent fluidized beds, Powder Technology, 62 (1990) 207–215.

Lewis W.K., Gilliland E.R., Bauer W.C., Characteristics of fluidized particles, Industrial & Engineering Chemistry, 41 (1949) 1104–1117.

Lim K.S., Zhu J.X., Grace J.R., Hydrodynamics of gas-solid fluidization, International Journal of Multiphase Flow, 21 (1995) 141–193.

Llop M.F., Casal J., Arnaldos J., Incipient fluidization and expansion in fluidized beds operated at high pressure and temperature, In: Large J.-F., Laguerie C. (Eds.), Fluidization VIII, Engineering Foundation, New York, 1995, pp. 131–138.

Lucas A., Arnaldos J., Casal J., Puigjaner L., High temperature incipient fluidization in mono and polydisperse systems, Chemical Engineering Communications, 41 (1986) 121–132.

Matheson G.L., Herbst W.A., Holt P.H., Characteristics of fluid-solid systems, Industrial & Engineering Chemistry, 41 (1949) 1098–1104.

Matsen J.M., Hovmand S., Davidson J.F., Expansion of fluidized beds in slug flow, Chemical Engineering Science, 24 (1969) 1743–1754.

McKay G., McLain H.D., Fluidization characteristics of cuboids, Industrial & Engineering Chemistry Process Design and Development, 19 (1980) 712–715.

Mii T., Yoshida K., Kunii D., Temperature-effects on the characteristics of fluidized beds, Journal of Chemical Engineering of Japan, 6 (1973) 100–102.

Mori S., Wen C.Y., Estimation of bubble diameter in gaseous fluidized beds, AIChE Journal, 21 (1975) 109–115.

Mori S., Hashimotot O., Haruta T., Mochizuki K., Matsutani W.,

Hiraoka S., Yamada I., Kojima T., Tuji K., Turbulent fluidization phenomena. In: Basu P., Large J.F. (Eds.), Circulating Fluidized Bed Technology II, Pergamon Press, Oxford, 1986, 75–87.

Murachman B., Hydrodynamique et transferts thermiques dans les lits fluidisés par les gaz, Institut National Polytechnique de Toulouse, 1990.

Nakamura M., Hamada Y., Toyama S., Fouda A.E., Capes C.E., An experimental investigation of minimum fluidization velocity at elevated temperatures and pressures, The Canadian Journal of Chemical Engineering, 63 (1985) 8–13.

Pattipati R.R., Wen C.Y., Minimum fluidization velocity at high temperatures, Industrial & Engineering Chemistry Process Design and Development, 20 (1981) 705–707.

Perales J.F., Coll T., Llop M.F., Arnaldos J., Casal J., The prediction of transport velocity in fast fluidized beds, Récents Progrès en Génie des Procédés: La Fluidisation, 1991a, pp. 47–53.

Perales J.F., Coll T., Llop M.F., Puigjaner L., Arnaldos J., Casal J., On the transition from bubbling to fast fluidization regimes. In: Basu P., Horio M., Hasatani M. (Eds.), Circulating Fluidized Bed Technology III, Pergamon Press, Oxford, 1991b, pp. 73–78.

Rhodes M.J., Geldart D., Transition to turbulence?. In: Ostegaard K., Sorensen A. (Eds.), Fluidization, vol. V, Engineering Foundation, New-York, 1986, pp. 281–288.

Richardson J.F., Incipient fluidization and particulate systems, In: Davidson J.F., Harrison D. (Eds.), Fluidization, Academic Press, New York, 1971, p. 26.

Rim G., Lee D., Bubbling to turbulent bed regime transition of ternary particles in a gas–solid fluidized bed, Powder Technology, 290 (2016) 45–52.

Rowe P.N., An X-ray study of bubbles in fluidized beds, Transactions of the Institution of Chemical Engineers, 43 (1965) 157–175.

Ruiz J.A., Juárez M.C., Morales M.P., Muñoz P., Mendívil M.A., Biomass gasification for electricity generation: review of current technology barriers, Renewable and Sustainable Energy Reviews, 18 (2013) 174–183.

Ryu H.-J., Lim N.-Y., Bae D.-H., Jin G.-T., Minimum fluidization velocity and transition velocity to fast fluidization of oxygen carrier particle for chemical-looping combustor, Korean Institute of Chemical Engineers, 41 (2003) 624–631.

Satija S., Fan L.-S., Characteristics of slugging regime and transition to turbulent regime for fluidized beds of large coarse particles, AIChE Journal, 31 (1985) 1554–1562.

Saxena S.C., Vogel G.J., The measurement of incipient fluidization velocities in a bed of coarse dolomite at temperature and pressure, Transactions of the Institution of Chemical Engineers, 55 (1977) 184–189.

Schnitzlein M.G., Weinstein H., Flow characterization in high-velocity fluidized beds using pressure fluctuations, Chemical Engineering Science, 43 (1988) 2605–2614.

Shabanian J., Chaouki J., Effects of temperature, pressure, and interparticle forces on the hydrodynamics of a gas-solid fluidized bed, Chemical Engineering Journal, 313 (2017) 580–590.

Shamlou P.A., Handling of Bulk Solids: Theory and Practice, Butterworths, 1988, pp. 20–50.

Stubington J.F., Barrett D., Lowry G., On the minimum fluidizing velocity of coal-derived chars at elevated temperatures, Chemical Engineering Science, 39 (1984) 1516–1518.

Svoboda K., Cermak J., Hartman M., Drahos J., Selucky K., Pressure fluctuations in gas-fluidized beds at elevated temperatures, Industrial & Engineering Chemistry Process Design and Development, 22 (1983) 514–520.

Tannous K., Contribution à l'étude hydrodynamique des lits fluidisés de grosses particules, Institut National Polytechnique de Toulouse, 1993.

Tannous K., Hemati M., Laguerie C., Characteristics of incipient fluidization and expansion of fluidized-beds of particles of Geldart category-D, Powder Technology, 80 (1994) 55–72.

Thonglimp V., Hiquily N., Laguerie C., Vitesse minimale de fluidisation et expansion des couches fluidisées par un gaz, Powder Technology, 38 (1984) 233–253.

Van Heerden C., Nobel A.P.P., Van Krevelen D.W., Studies on fluidization. I—the critical mass velocity, Chemical Engineering Science, 1 (1951) 37–49.

Wen C.Y., Yu Y., Mechanics of fluidization, Chemical Engineering Progress Symposium Series, 62 (1966) 100–101.

Werther J., Influence of the bed diameter on the hydrodynamics of gas fluidized beds, AIChE Symposium Series, 70 (1974) 53–62.

Yates J.G., Effects of temperature and pressure on gas-solid fluidization, Chemical Engineering Science, 51 (1996) 167–205.

Yerushalmi J., Turner D.H., Squires A.M., The fast fluidized bed, Industrial & Engineering Chemistry Process Design and Development, 15 (1976) 47–53.

Yerushalmi J., Cankurt N.T., Further studies of the regimes of fluidization, Powder Technology, 24 (1979) 187–205.

Appendix A: Bubble fraction estimation

The bubble fraction in the bed δ_B can be estimated from the following equations (Davidson and Harrison, 1963; Mori and Wen, 1975):

$$\delta_B = \frac{U - U_{mf}}{U_b} \tag{A1}$$

$$U_b = (U - U_{mf}) + 0.711 \cdot \left(g \cdot \overline{d_B}\right)^{\frac{1}{2}} \tag{A2}$$

$$\overline{d_B} = d_{Bm} - (d_{Bm} - d_{B0}) \cdot \exp\left(-0.3 \cdot \frac{\frac{H}{2}}{D_t}\right) \tag{A3}$$

$$d_{Bm} = 0.64 \cdot \left[A_c \cdot (U - U_{mf})\right]^{0.4} = C_{11} \cdot (U - U_{mf})^{0.4} \tag{A4}$$

$$d_{B0} = \frac{1.30}{g^{0.2}} \cdot \left(\frac{U - U_{mf}}{N_{or}}\right)^{0.4} = C_{12} \cdot (U - U_{mf})^{0.4} \tag{A5}$$

where C_{11} and C_{12} are numbers depending on reactor and gas distributor geometry. Combining Equations A3 to A5 gives the bubble mean diameter, dependent only on the excess gas velocity, as:

$$\overline{d_B} = (U - U_{mf})^{0.4} \cdot \left[C_{11} - (C_{11} - C_{12}) \cdot \exp\left(-0.3 \cdot \frac{\frac{H}{2}}{D_C}\right)\right] \tag{A6}$$

Then, a combination of Equations A1, A2 and A6 shows that average bed voidage depends only on excess gas velocity.

Authors' Short Biographies

Sébastien Pecate

Sébastien Pecate holds a PhD (2017) in process engineering, and more precisely on "Biomass Gasification in an FICFB". He worked as a research engineer on biomass and sludge gasification at LGC from 2014 to 2018. He is now working on solid waste thermal treatment (incineration, pyrolysis, gasification, combustion) for waste to energy, waste to fuels and waste to chemicals applications.

Mathieu Morin

Dr. Mathieu Morin studied chemical engineering processes at the University of Toulouse, France, where he received his PhD degree on "Biomass Gasification in Circulating Fluidized Bed" in 2017. During his PhD thesis, he particularly developed experimental and modeling tools in order to study the chemical reactions occurring during biomass conversion (pyrolysis, gasification, combustion, catalytic cracking and reforming of tar). Currently, Dr. Mathieu Morin is working at IFPEN in Lyon, France, at the Department of Process Design and Modeling. His main topics are the development of processes for the production of environmental fuels, chemical intermediates and energy from fossil and renewable resources.
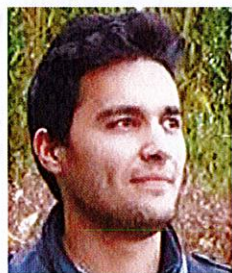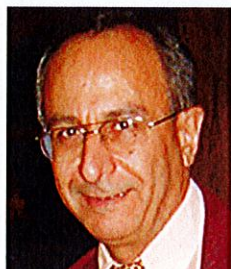
Sid Ahmed Kessas

Sid Ahmed Kessas is a second-year PhD student who graduated in chemical engineering in 2016 and who worked on:
- Characterization of biomass.
- Reactivity and kinetics of steam gasification & combustion.
- Synthesis of catalyst in a fluidized bed.

Authors' Short Biographies

Mehrdji Hemati

Mehrdji Hemati is a professor in chemical engineering at the ENSIACET-INP in Toulouse. His research activities focus on three items:

- ➤ Hydrodynamics and transfers in dense and circulating fluidised beds. Two approaches were developed: the experimental approach and the theoretical approach.
- ➤ Application of fluidised beds in the field of chemical reaction gathering catalytic reactions, gas-solid reactions (biomass and sewage sludge pyrolysis, gasification and combustion).
- ➤ Processes for elaboration of materials gathering: drying, mixing, size enlargement by spray coating and granulation, dry impregnation in F.B.

He is author and co-author of more than 100 publications in international scientific journals.

Yilmaz Kara

Yilmaz Kara is a process engineer working on biomass gasification, fluidized beds, REFIOM vitrification and many other subjects related to energetic valorization. He is also an expert on green gas production and treatment, and flow assurance.

Sylvie Valin

Sylvie Valin holds a PhD (1999) in energetics from the Institut National Polytechnique de Grenoble (France). She has been working as a research engineer on biomass gasification at CEA since 2004. Her research activity mainly concerns biomass and waste pyrolysis and gasification for energy application, coupling experimental and modelling approaches from particle to reactor scale. She especially works on gasification in high-temperature reactors (fluidised bed, entrained flow reactor).